Characterization of SimulCam, a standoff Raman system for scientific support of SuperCam operations on Mars

Jose A. Manrique [a,b,*], Guillermo Lopez-Reyes [a], Marco Veneranda [a],
Aurelio Sanz-Arranz [a], Juan Sancho Santamaria [a], Sofia Julve-Gonzalez [a]
Ivan Reyes-Rodríguez [a], Teresa Fornaro [c], Juan Manuel Madariaga [d], Gorka Arana [d],
Kepa Castro [d], Ivair Gontijo [e], Ann M. Ollila [f], Shiv K. Sharma [d], Roger C. Wiens [g],
Sylvestre Maurice [b], Fernando Rull-Perez [a], And the SuperCam Raman Working Group

[a] *GIR ERICA, Universidad de Valladolid, Spain*
[b] *Institut de Recherche en Astrophysique et Planétologie, Toulouse, France*
[c] *INAF, Italy*
[d] *Universidad de País Vasco, Bilbao, Spain*
[e] *Jet Propulsion Laboratory, Pasadena, United States*
[f] *Los Alamos National Laboratory, NM, United States*
[g] *Purdue University, IN, United States*

Abstract

During the development activities of SuperCam Calibration Target, target intended for one of the two first Raman instruments to be deployed on another planetary body, our group developed a laboratory instrument that could simulate to some extent the Raman capabilities of one of such instruments and could provide data with similar quality. The use of this kind of laboratory instruments has demonstrated its utility in the evaluation of potential calibration targets or anticipating the science outcome that an instrument could provide. The present work describes our laboratory setup to support SuperCam, evaluating similarities between both instruments, despite of differences in the hardware. Evaluation of data gathered by SuperCam on Mars and the availability of one replica of SuperCam's Calibration Target allowed the comparison on the same set of targets, demonstrating how similar Signal-to-Noise Ratio (SNR) could be achieved from both instruments. The higher energy per pulse on SimulCam is compensated by a greater analytical footprint and the use of smaller collection optics. The results show how spectra obtained at representative distances of SuperCam are comparable. Operational principles are also comparable in terms of time resolution, and close in terms of spectral resolution.

This similarity has allowed different science support works using SimulCam data, as well as the support to Mars detections using our setup. We provide examples of this support that will be shared with the community in different papers, as well as examples of possible operations activities that could benefit from experiments performed with SimulCam. We show how this setup can complement the two laboratory replicas in Los Alamos and Toulouse in providing support data to different experiments.

---

* Corresponding author.
 E-mail address: Joseantonio.manrique@uva.es (J.A. Manrique).

1. Introduction

The SuperCam instrument onboard the Perseverance Rover (Farley 2020) is a multi-analytical suite that is currently investigating the geological units of the Jezero Crater. SuperCam is composed of a Body Unit (Wiens et al., 2021), a Mast Unit (Maurice et al., 2021) and a Calibration target (SCCT) (Manrique et al., 2020; Cousin et al., 2022; Madariaga et al., 2022), the specifications of which are provided elsewhere. SuperCam is a pioneering tool, as it provides the unprecedented opportunity to combine the use of five co-aligned techniques: Remote Micro-Imaging (RMI), Laser-Induced Breakdown Spectroscopy (LIBS), Time-Resolved Raman and Luminescence (TRR/L), Visible-Infrared Spectroscopy (VISIR), and sound recording (MIC).

Except for LIBS, which has been used on the surface of Mars since 2012 by Curiosity (Maurice et al., 2012; Wiens et al., 2012), SuperCam is the first instrument to use in-situ VISIR spectroscopy on the Mars surface, the first to record sounds (Maurice et al., 2022) and to perform standoff Raman analyses beyond Earth (Wiens et al., 2021). Focusing on Raman spectroscopy, this is one of the two first Raman instruments deployed on another planetary body, and the first one to acquire an extraterrestrial Raman spectrum.

Among the mentioned techniques, the development of Raman spectroscopy in a standoff configuration represents a high technological challenge due to the low cross section of the Raman effect, meaning that most of the photons used for excitation are scattered through other processes, mainly Rayleigh Scattering, resulting in a low photon budget for Raman detection. Furthermore, the resource constraints (e.g., mass and power) associated to the development of stand-off Raman instruments for space applications means that their expected performance is not comparable to state of the art laboratory instruments, or even other Raman instruments for planetary exploration that operate in contact like SHERLOC (Scanning Habitable Environments with Raman and Luminescence for Organics and Chemicals), RLS (Raman Laser Spectrometer) and RAX (Raman Spectrometer for MMX) (Rull et al., 2017; Bhartia et al., 2021; Cho et al., 2021). Having laboratory instruments capable of emulating to some extent the scientific outcome of SuperCam could play an important role in the interpretation of the spectral data received from Mars. Similar developments were done by our group for RLS (Lopez-Reyes et al., 2022) that helped in the development of the instrument and provided a base for several works of scientific support to RLS (Veneranda et al., 2019, 2020, 2021).

To fulfill this need, the SuperCam team can rely on the use of two SuperCam laboratory models (operating in Los Alamos, USA and Toulouse, France) to perform studies on Earth that are meant to enhance the scientific outcome of the data returned from Mars (e.g. by optimizing the mineralogical interpretation of the interrogated targets and by enhancing the semi-quantitative estimation of their chemical composition). In addition to those, the SuperCam science team is also relying on the laboratory emulator recently developed by the ERICA research group (University of Valladolid). Named SimulCam, this instrument is used as a heavy-duty tool that closely emulates the Raman analysis by SuperCam, while enabling complementary, co-aligned, Time-resolved luminescence and LIBS analysis.

As this instrument is meant to increasingly support the activities of the SuperCam Science Team this manuscript details the characteristics of SimulCam and highlights its similarities and differences with SuperCam. In this sense, the present manuscript is organized as follows: at first, the hardware specifications of SimulCam are evaluated and compared to the SuperCam instrument. After describing the characterization activities carried out to calibrate the instrument, relevant examples on how the SimulCam instrument is supporting the scientific activities of SuperCam are also provided.

2. Materials and methods

2.1. Description of the SimulCam instrument

SimulCam instrument is made from commercial components, off the shelf. The pulsed laser is a Litron Nano S, optically pumped by flash lamp, with a Second Harmonic Generator (SHG) module that also filters the 1064 nm line. This laser provides pulses of 532 nm with an energy of 120 mJ and a pulse width of 6 ns. The laser can operate at different repetition rates up to 30 Hz and can adapt its power electronically between a 60 % and a 100 %. A beam expander with variable divergence from Edmund Optics is used to adapt the irradiance, thus allowing the beam diameter on the target to be varied. On the collection optics side SimulCam uses a Canon SLR (Single Lens Reflex) objective, with a focal length of 300 mm and a f ratio of 4. This objective is attached to a Raman probe from Spectra Solutions where the Rayleigh photons are separated from the Raman photons through an edge filter. The collected light is then carried to the spectrometer through an optical fiber from FiberTech Optica, which was the provider of SuperCam's optical fiber to connect the Mast Unit and the Body Unit. This fiber is a bundle of seven individual fibers of 40 µm that are in a round configuration at the telescope side, and in linear configuration on the spectrometer side. SuperCam uses a similar approach.

For the spectrometer SimulCam uses a Holospec spectrometer from Kaiser Optical Systems. This spectrometer is a transmission spectrometer, as is the one in SuperCam that deals with Raman signal and uses a two-track holographic grating. This kind of gratings allows, through holographic design of the diffraction element, the projection of two parallel tracks on the detector, each one covering a different wavelength range. The resulting grating allows a wider coverage on the detector without loss of resolution. The spectrometer uses no slit, so the entrance "slit" is in

fact the 40 µm diameter of the individual cores of the fiber bundle, and no previous filtering is used. The detector is an intensified camera Andor iStar iCCD, with 2048 pixels width, although the 25 mm intensifier tube doesn't cover the whole CCD chip, and a small number of pixels remain not illuminated. The whole system, thanks to the multi-track grating, can measure from 130 up to 4000 cm^{-1} in a single acquisition.

Schematics, along with a picture of the system are shown in Fig. 1. Where the decoupled excitation and collection path can be seen.

2.2. Analytical targets

Leading the development of the SCCT (Manrique et al., 2020), the ERICA research group has access to the
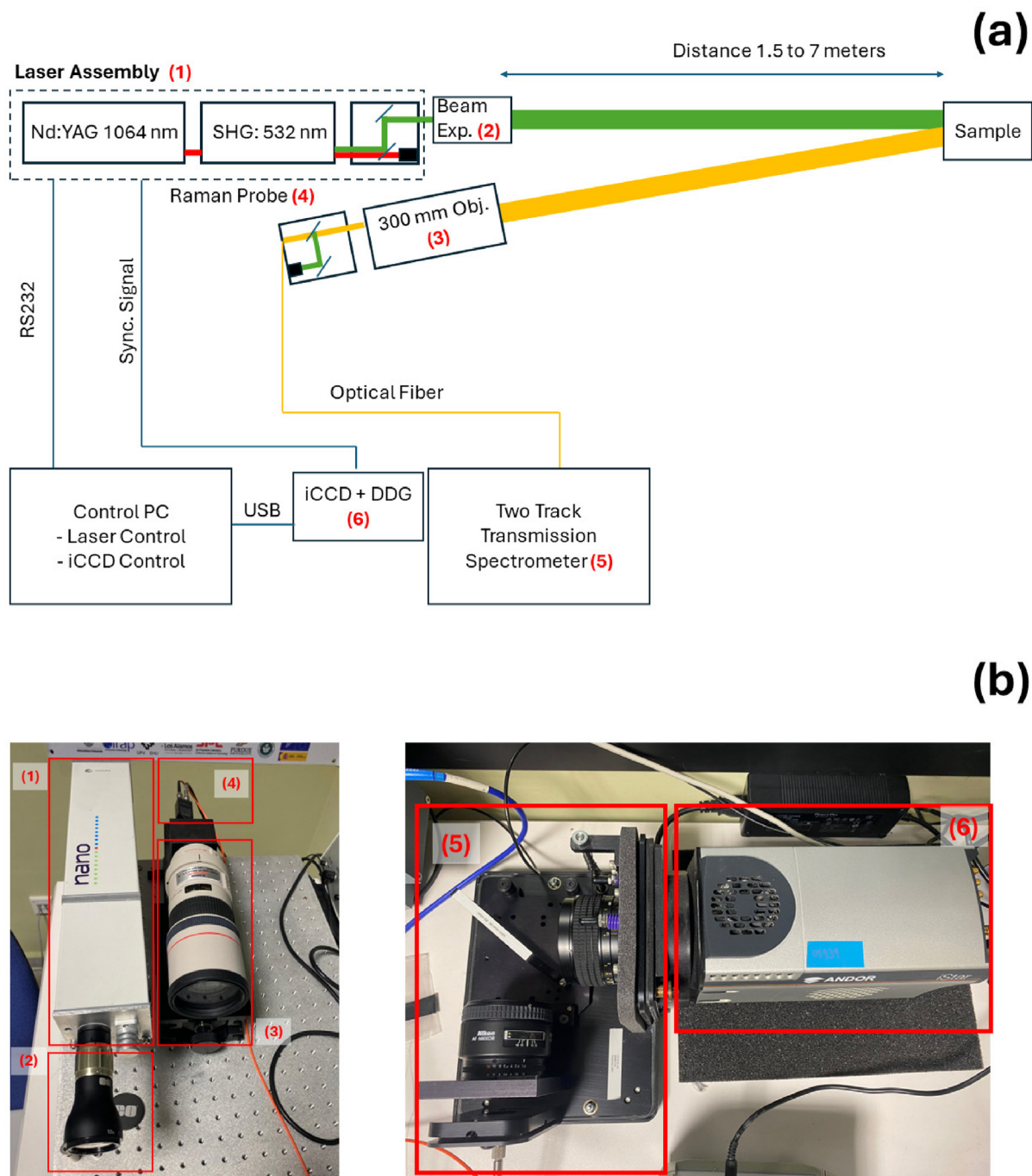

Fig. 1. (a) Shows the schematic diagram of SimulCam instrument, with details in (b) for the laser assembly (1), beam expander (2), and the collection optics comprised of the 300 mm objective (3) and the Raman probe for Rayleigh filtering (4). The laser assembly includes the laser providing the fundamental 1064 nm. emission, the Second Harmonic Generator (SHG) where the 532 nm emission is generated, and the filtering box to separate the 532 nm from the residual 1064 nm laser. For the light analysis, detailed picture of the transmission spectrometer without the optical cover (5) and the detector integrating the intensified CCD (iCCD) and the Digital Delay Generator (DDG) for the synchronization with the laser (6).

Qualification Model (QM) of this component as well as to several of the mineralogical samples that were analyzed by SuperCam before launch.

Having this in mind, characterization and science support activities described in this work were based on the analysis of materials that were characterized by the flight model of SuperCam either on Earth or after landing on Mars.

Among the available targets, the Raman analyses described here were performed on the following targets:

- Diamond: as described elsewhere (See target 0.1 in (Manrique et al., 2020)), this target was included in the SCCT as it provides a quick, high SNR and stable spectrum that can be used by SuperCam to check the health of the system and evaluate the emission of the laser.
- Apatite: In spite of being included in the SCCT as a LIBS target (target 2.5 in (Manrique et al., 2020)), this mineral sample can also be used for Raman analyses due to the high Raman cross section and high signals it provides (despite of the partial loss of crystallinity that occurred during the sintering process).
- Calcite: As for apatite, this sample is also included in the SCCT as LIBS target (target 2.3 in (Manrique et al., 2020)).
- Marble slab (Fig. 2): Provided by the University of the Basque Country, this material was analyzed by Super-Cam as part of the assembly and testing activities. The homogeneity of this sample was evaluated with the analytical protocol described in (Madariaga et al., 2022), the homogeneity of the slab is assured by Raman and XRF imaging analyses down to 300 μm, as was required for SuperCam targets. This assessment is summarized in Fig. 2, where the value of the first Principal Component (PC1) of all spectra collected in a hyperspectral image is superposed to the optical image of this sample. The PC1 contains the spectral information of calcium carbonate and shows how at the scale required by SuperCam this sample is homogeneous.
- White paint: This silicon-based paint was used for the painting of the Rover and the SCCT (target 0.6 in (Manrique et al., 2020)) and is periodically analyzed by SuperCam on Mars to monitor possible degradation mechanisms on Mars.

Beyond Raman analyses, further targets were also analyzed to test the luminescence and spectral coverage of SimulCam. On one hand, LIBS analyses were performed on the titanium plate of the SCCT-EQM (environmental qualification model), which is used for calibration purposes (see section 3.2.1).

An additional target that is present in the SCCT is the organic sample that is analyzed to evaluate the evolution of organics on Mars. For support experiments, we analyzed different samples of Ertalyte, commercial name of
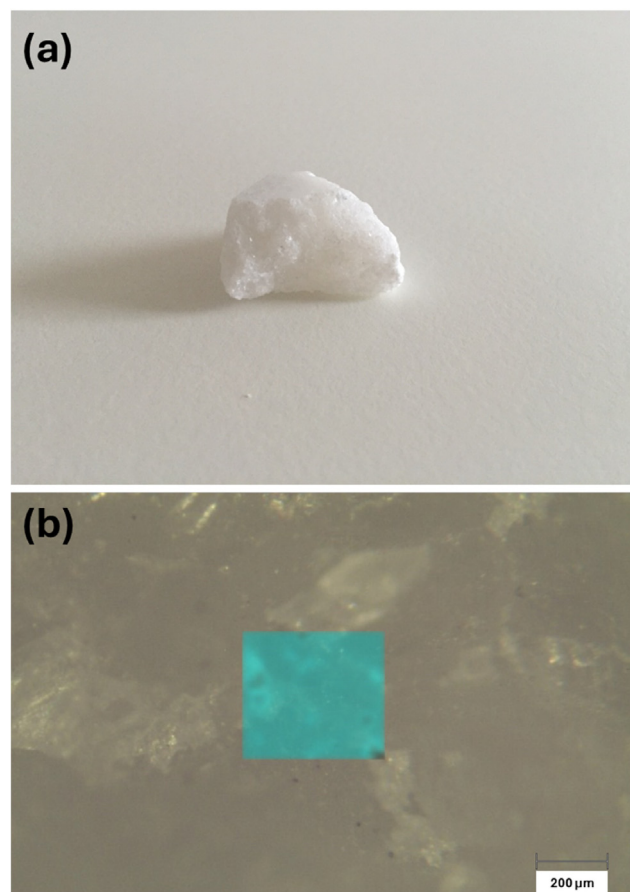

Fig. 2. The marble slab was evaluated using Raman imaging techniques (a), Its homogeneity was assessed down to 300 μm using Raman imaging technique (Renishaw InVia, 532 nm excitation), as was required for any potential calibration target of SuperCam. In the detailed picture we highlight the first Principal Component in a PCA (in blue) in a 300 μm square area.

the polyethylene terephthalate (PET) with 100 % crystallinity.

On the other hand, luminescence analyses were performed on apatite and calcite standards proceeding from the Analytical Database of Martian Minerals (AdaMM) (Veneranda et al., 2022).

SHERLOC instrument (Bhartia et al., 2021) detected the presence of possible organics associated with different lithologies on Mars (Scheller et al., 2022). In such geological targets these organics could increase the luminescence background in Raman spectra, providing an interesting parameter in the identification of potential organic compounds on Mars. To this purpose, SimulCam has performed different analyses of mixtures of different biomarkers and different mineral substrates as part of wider work to be published by T. Fornaro et al (in preparation). The aim of this work focuses, among other things, on the evolution of luminescence background detected by SuperCam on different targets on Mars.

3. Results

3.1. Comparison of main hardware specification between SimulCam and SuperCam

3.1.1. Excitation source

The SuperCam's excitation source is a passively cooled Diode Pumped Solid State (DPSS) laser. In the low-density atmosphere of Mars, this implies that a limited number of laser shots can be achieved before needing to stop for cooling to avoid damages in the laser. The number of consecutive laser shots is not an issue for the water-cooled laser in SimulCam, which makes it an excellent heavy duty analytical tool to perform support science.

Another difference between the two setups is the irradiance on the sample, given the high difference in the energy per pulse between the two lasers. SuperCam delivers the laser in a collimated beam, which means that power density is relatively constant for all the operation distances. SimulCam can adapt the spot size and the power of the laser to deliver a wide variety of power densities to the target.

3.1.2. Collection optics

SimulCam uses a smaller optical system than Super-Cam, which implies a lower ability to collect the generated Raman spectrum. In addition to that, the focal distance is also different, which directly affects the analytical footprint, or FOV. In general, SuperCam has a larger laser spot size than analytical footprint. This characteristic can be mimicked by SimulCam. Nevertheless, the analytical footprint of both instruments is expected to be larger than the size of the individual grains of the samples, and Raman data from both instruments will be more representative of the average composition of the target and not individual crystals.

3.1.3. Spectrometer

Concerning the spectral coverage, the SuperCam instrument uses a three-track holographic grating system that projects photons up to 850 nm / 7032 cm^{-1}. Compared to this, SimulCam uses only two tracks, thus reaching 690 nm / 4304 cm^{-1}). This difference doesn't affect Raman analyses, as the vibrational features of both organic and inorganic compounds fall within the SimulCam range. However, Resolved Luminescence is partially affected, as some fluorescence signals lie in the range between 690 and 850 nm. Regarding LIBS analyses, trying to mimic or emulate SuperCam's LIBS capabilities would require, to start with, to exactly mimic the irradiance on the target and to perform the analyses in a controlled atmosphere. SimulCam was intended to focus on Raman, and because of that, the analysed spectral range would be highly insufficient for LIBS analyses. Although spectral lines of Si, Ca, Li, Na and Ba could lie in the range covered by Simul-Cam's main spectrometer, the detection of other elements would be highly impaired. However, for certain analyses, and after considering the lack of representativity of Super-

Cam's LIBS analyses, a second objective can be coupled to an Echelle spectrometer, providing coaligned measurements of Raman and LIBS analyses under terrestrial conditions, with a LIBS spectral range between 250 and 850 nm.

The detectors mounted in the two instruments are both able to integrate several discharges of the intensifier in one readout of the CCD (coadds), thus allowing to split a limited amount of laser shots into coadds (discharges of the intensifier per CCD readout) and accumulations (CCD readouts to be averaged).

A summary of the main hardware specification of the two setups is provided on Table 1.

3.2. SimulCam calibration and acquisition parameters optimization

Some of the instrumental differences highlighted in section 3.1can be balanced by optimizing the acquisition parameters of SimulCam. In this sense, the present section describes the laboratory activities carried out to improve the scientific outcome of SimulCam, so that it could better emulate the Raman spectra collected by SuperCam on Mars.

3.2.1. LIBS spectroscopy

As a simulation of a possible LIBS calibration check on Mars, SimulCam was used to analyze the titanium plate mounted by the SCCT (Manrique et al., 2020). As titanium provides many emission lines distributed throughout the analysed spectral region (see Fig. 3), these features are used by the SuperCam team to calibrate the position of the different wavelengths in the pixels of the detector. For Simul-Cam we take advantage of this high density of features to evaluate the wavelength coverage in the two tracks of the spectrometer. On the other hand, the acquired spectrum can be then compared, for example, to the spectrum collected by SuperCam on the same target during sol 444 (this is the 444th ''Martian Day'' of mission, as a full rotation of Mars takes slightly longer than a full rotation of Earth).

For *the acquisition with SimulCam, d*ue to different plasma dynamics under different atmospheric pressures as compared to Mars, we evaluated different gate delay times, covering 0, 1, 2 and 3 microseconds. In the calibrated spectrum shown in Fig. 3 we selected the one with the highest SNR (1 microsecond delay). To induce the plasma we reduced the spot size to its minimum (under 1 mm diameter). Gating was of 8 microseconds and laser was set to its 90 % of power (~108 mJ per pulse).

As mentioned in section3.1.3, the different spectrometers in the two instruments cover different spectral ranges, with SimulCam reaching 690 nm, while SuperCam goes up to 850 nm. In SimulCam the intensifier is round with a diameter of 25 mm while the CCD is an array of 2048 pixels of 13.5 μm each, reducing the effective sensor width to 1850 pixels. This difference introduces some step cuts in the spectrum at both sides of the detector. This can be observed in

Table 1
Main hardware specification of SuperCam and SimulCam instruments.

	Feature	SuperCam*	SimulCam
Laser	Energy per pulse	12 mJ	Up to 120 mJ
	Pulse length	3–4 ns	6 ns
	Repetition rate	Up to 10 Hz	Up to 30 Hz
	Beam shape	Collimated	Uncollimated
	Power density	30 kW/mm2	Variable
Collection optics	Optical design	Schmidt-Cassegrain	Refractive objective
	Clear aperture	110 mm	75 mm
	Focal distance	700 mm	300 mm
	Numerical Aperture	0.078	0.125
Spectrometer	Grating and detection	Transmission, three track, F/4	Transmission, two track, F/1.8
	Detector	Intensified CCD	Intensified CCD
	Number of channels	2048	2048
	Gate widths	From 100 ns	From 3 ns
	Gate delay	Adjustable	Adjustable
	Integrate on Chip	Available	Available
	Spectral coverage	532 to 850 nm	532 to 690 nm
		0 to 7032 cm^{-1}	0 to 4304 cm^{-1}
	Analytical FOV (size in mm @ 2 m)	0.74 mrad	1.6 mrad.
		1.48 mm	3.2 mm
	Laser spot	Collimated, 8.4 x 9.3 mm on target	Variable.

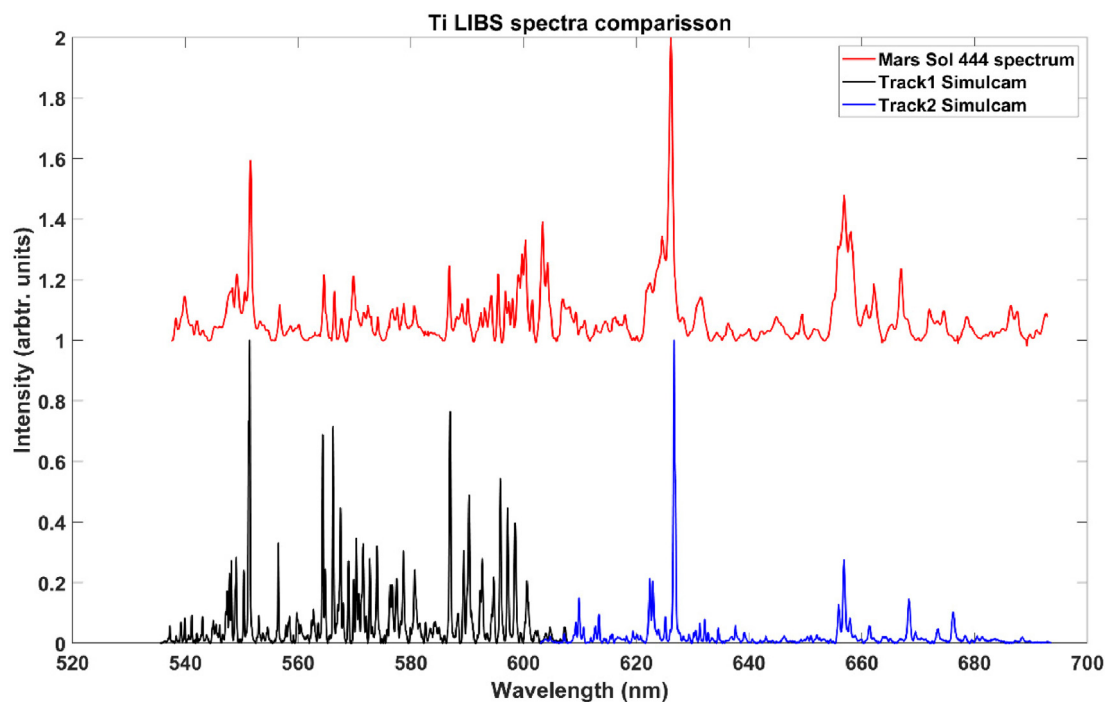* (Maurice et al., 2012; Wiens et al., 2021).

Fig. 3. LIBS spectra of the Titanium plate mounted on the SCCT, collected by SimulCam (on Earth) and SuperCam (on Mars, during sol 444). Continuum was removed in both spectra.

Fig. 4, where, in red, we depict the coverage of the intensifier tube. Other effects can be observed as well, as the region marked as A the same figure, which corresponds to the longpass filter in the collection optics, which prevents Rayleigh scattered photons to reach the detector. This filter is supplied with a cutoff Raman shift of 100 cm^{-1}, although attending to the intensity of the continuum of the titanium LIBS spectra, or the luminescence is some of the Raman Spectra, the filter cut-off reaches the 130 cm^{-1}. Other region marked as B in the same figure shows a gradual loss of efficiency in the detector from 4000 cm^{-1}, as the quantum efficiency of both, the intensifier and the CCD, decays for longer wavelengths.

Variation in atmospheric conditions, laser power and wavelength could affect the temperature of the generated plasma as well as its expansion and cooling dynamics. Hav-
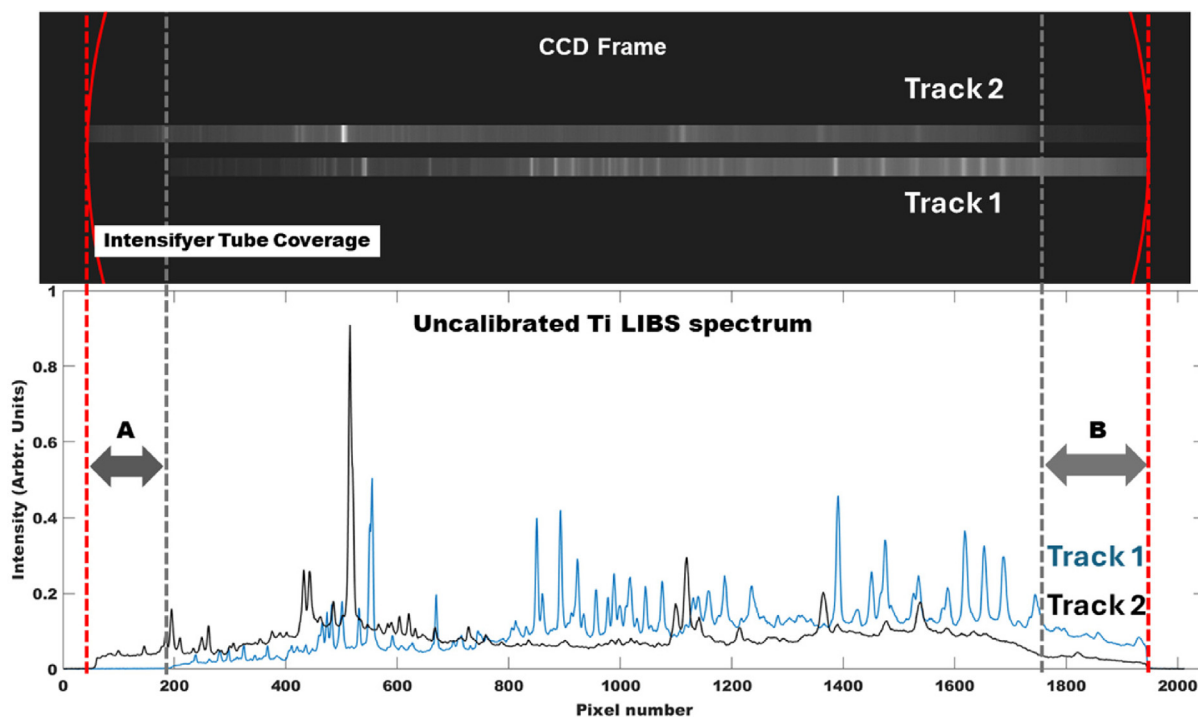
Fig. 4. Above, a frame of the CCD with the two tracks masked. Borders of the intensifier tube are depicted in red, showing how this element doesn't cover the whole CCD array. In the spectra (below) this can be observed as two step cuts in the recorded spectra. In this case the spectrum shown is a LIBS spectrum of the titanium plate setting the delay to zero, maximizing the continuous background. Region marked with A, in Track 1 corresponds to the edge filter in the collecting optics, while the region marked as B in Track 2 shows a decrease in sensitivity in this region.

ing this in mind, as well as the fact that SimulCam is not corrected for Instrument Response Function (IRF), spectra from both instruments are only comparable in terms of spectral coverage, and slightly in terms of the width of the lines if we assume that the width of the lines is below the resolution of the instrument. Indeed, different temperatures of the plasma can change the intensity ratios between different emission lines, while the presence of Earth's atmosphere induces broadening in these lines, due mainly to Stark and Doppler broadening, depending on the plasma temperature and electron density (Effenberger et al., 2010). These effects minimize the utility of SimulCam for SuperCam-like LIBS data, and the main reason why the instrument is only intended for Raman scientific support.

3.2.2. Raman spectroscopy

As Raman shift is a relative magnitude, Raman calibration needs to consider the wavelength of the excitation source. For both instruments, direct measurement of the wavelength of the laser is not possible due to the interferometric filters in the collection optics, meaning that indirect measurements are required to assess the wavelength of the excitation laser. As a simulation of a possible Raman calibration check on Mars, SimulCam was used to analyse the diamond target mounted by the SCCT (Manrique et al., 2020). As displayed in Fig. 5, the diamond provides a very strong Raman peak (1332 cm^{-1}) whose position, shape and intensity values can be considered fixed in the range of temperatures and pressures of the mission. As such this target

is used by the SuperCam team to evaluate the wavelength of the excitation laser and to perform the conversion of wavelengths (hence, pixels) to Raman shift units (cm^{-1}).

From the analysis of the SimulCam spectrum provided in Fig. 5, the maximum intensity of the diamond main peak is located at 572.6 nm. With this information and considering a Raman shift of 1331.82 cm^{-1} for the main band of the diamond (RRUFF database and previous measurements with benchtop instruments), the wavelength of the excitation laser was estimated to be of 532.08 nm. By analysing the FWHM of this band, the spectral resolution of the two instruments can also be compared, given that in both cases the intrinsic width of the diamond is well below the instrumental resolution (Sharma et al., 2023). As such, the SimulCam instrument operating under terrestrial environmental conditions ensures a resolution of 8.12 cm^{-1}, while the FWHM value inferred for SuperCam from the diamond spectrum collected on Mars during sol 13 is 14 cm^{-1}. This resolution can be changed by different means, in post treatment of data or by changing the collection fibre. This resolution difference has, however, a limited impact in the support activities given two main factors. On one hand, the possible shift in Raman features due to compositional changes are also assessed by LIBS data, and more important, the low SNR of most of the Raman features observed on Jezero Crater impacts the position of peaks much more than possible effects of resolution. In general, it was preferred to work with the flight-like optical harnessing despite of the mismatch of the limit resolution.
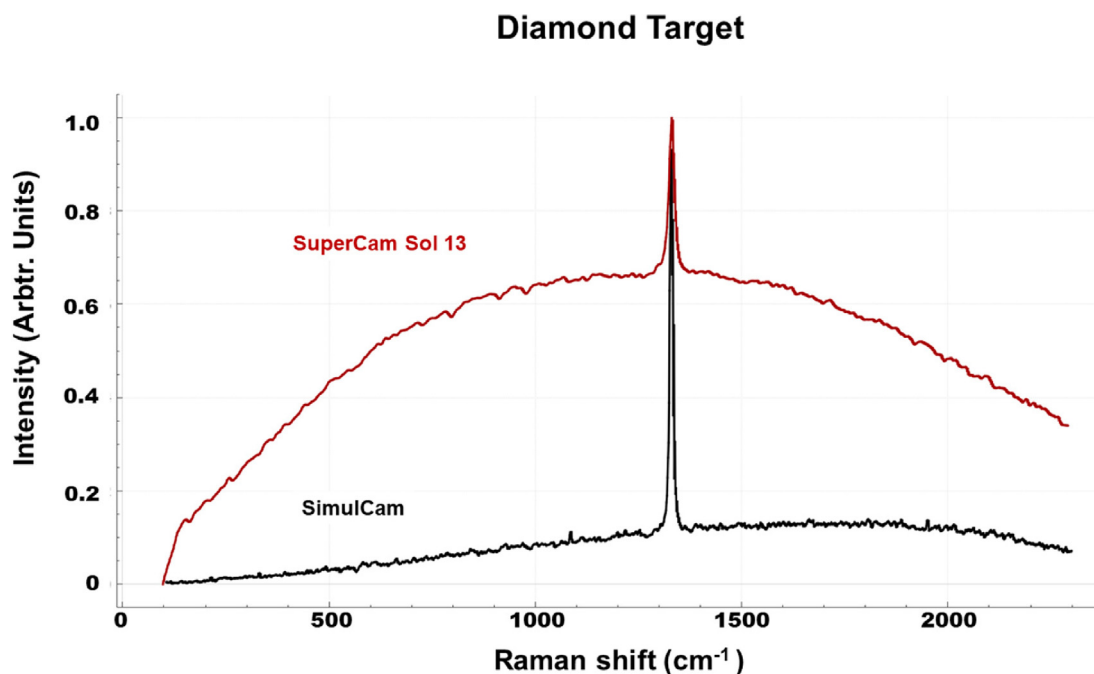
Diamond Target

Fig. 5. Raman spectra of the diamond target mounted on the SCCT, collected by SimulCam (on Earth) and SuperCam (on Mars, during sol 13).

The modularity of the whole instrument allows a quick substitution of the optical harness by another with wider cores that may help replicate the final resolution of SuperCam.

The comparison provided in Fig. 5 also highlights that the SuperCam spectrum collected on Mars presents a much higher background compared to the one collected by SimulCam. Considering that this background is also higher than the one measured by SuperCam before launch, it can be inferred that this background could be related to the exposure of the diamond assembly to the Martian environment. Indeed, effects of UV radiation in different minerals have been described (Royer et al., 2024), and in addition to these effects, the fact that diamond is transparent to UV radiation could allow the UV-ageing of the adhesive used for the assembly.

3.2.3. Optimization of power density

The two instruments have different approaches to deliver the energy of the laser pulse to the target, different energy per pulse, and different collection optics. On one hand, SuperCam has a "fixed" irradiance with distance, as the green laser for Raman is collimated. SuperCam's beam is of 8.4 * 9.3 mm on target, with a power density of ~ 30 kW/mm^2 (Maurice et al., 2021). On the other hand, SimulCam uses a variable beam with the ability to adapt the size of illuminating spot, but also has the option to electronically attenuate the laser power down to a 60 %, which allows it to achieve a wide variety of power densities. Table 2 shows the power densities calculated for different beam diameters and attenuations of the power of the laser.

From Table 2 it can be inferred the nominal power density of the SuperCam instrument can be generally emulated

by setting a spot diameter ≥ 11 mm and by setting the laser to low power values. This parameter is key, especially when considering possible alterations of the target due to the laser power. Nevertheless, in terms of the generation of Raman-scattered photons, the parameter to be evaluated is the energy density, attending to the total number of photons per laser event that, in the end, will be more closely related to the available Raman photons. In terms of this magnitude and given that the pulse width in SimulCam doubles that from SuperCam, energy density differences double when compared to power densities. However, differences in the ability to collect the generated signal play an additional role in the emulation of SuperCam's results. The lower aperture of the telescope of SimulCam makes necessary the use of higher energy densities to produce enough photons back to be detected.

3.2.4. Optimization of gain values

After setting the spot diameter to 11 mm and the laser power to 65 % (power density of 137 kW/mm^2), the marble slab described in section 2.2 was investigated by SimulCam by using different gains while keeping constant the number of accumulations and coadds (100 accumulations of one coadd). As a result, Fig. 6 shows that the SNR constantly increases until a gain value around 2500 (arbitrary units, as provided by the manufacturer). This SNR was calculated as the ratio between the intensity of the evaluated signal (after baseline subtraction) and the Standard Deviation of the intensity in a noise range wider than 200 cm^{-1} spectrally close to the evaluated signal. Within this range, the SNR value is very similar to the SNR calculated through the spectra collected by SuperCam from the same sample prior to launch (400 vs 427). Higher gains cause saturation

Table 2

Power density delivered by SimulCam combining different spot diameters and power % values.

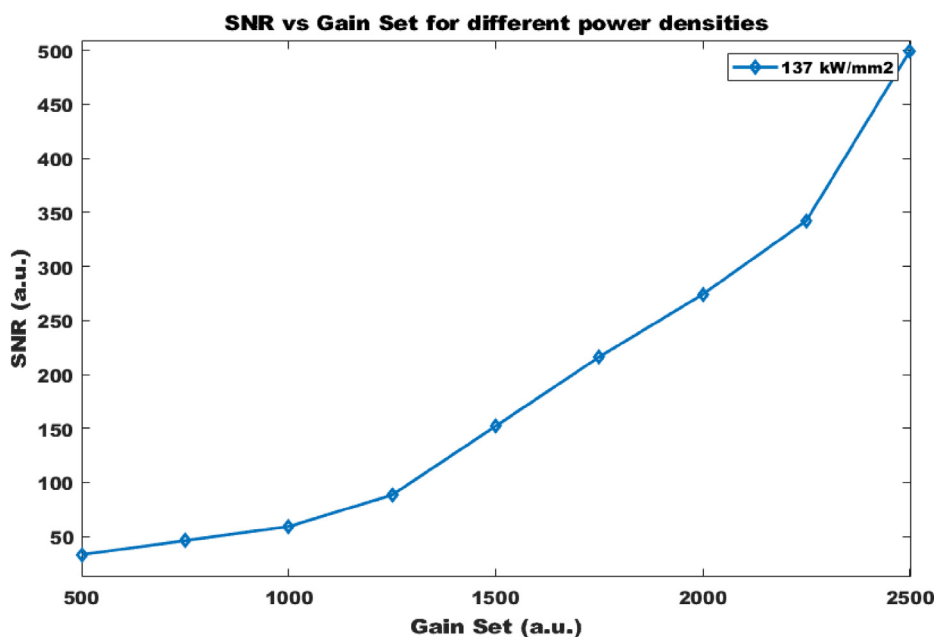| Beam Diameter (mm)	Power Density at 60 % of Power (kW/mm^2)	Power Density at 80 % of Power (kW/mm^2)	Power Density at 100 % of Power (kW/mm^2)
3	1697.65	2263.54	2829.42
5	611.15	814.87	1018.59
7	311.81	415.75	519.69
9	188.63	251.50	314.38
11	126.27	168.36	210.45
13	90.41	120.54	150.68
15	67.91	90.54	113.18
17	52.87	70.49	88.11
19	42.32	56.43	70.54

Fig. 6. SimulCam evolution of the SNR from the main peak of the marble slab as a function of the gain value using a power density of 137 kW/mm^2.

of the detector and the decrease of SNR. In the intensified detector the noise sources inherent to the CCD are present, as shot noise, dark current, readout noise or electronic noise, and in addition to these sources, inherent noise from the intensifier is added, as its own shot noise or effects of the gain and electronic noise.

3.2.5. Evaluation of time resolved capabilities

Both instruments are capable of performing Time Resolved Raman Spectroscopy. However, while SuperCam goes down to 100 ns gate width (Wiens et al., 2021), Simul-Cam was tested to provide quality spectra down to 3 ns gate width. For discrimination of certain fluorescence signals the use of a wider gate could be compensated adapting the gate delay, and time resolved studies can be achieved by moving the window of acquisition. Different delay sweep experiments were done in SimulCam, similar to those performed for SuperCam (Fig. 29 in Wiens et al. 2021), by changing the delay of the intensifier discharge with the laser firing. For SimulCam, this can be performed by using two different gate widths, 3 ns and SuperCam's 100 ns (see Fig. 7).

By comparison with SuperCam (Fig. 29 in(Wiens et al., 2021)) it can be noted how the SuperCam slope is less steep, indicating differences in the rise time of the intensifier (12–14 ns for SimulCam and 40 ns for SuperCam). In the case of the intensifier decay time, this value is typically affected by the phosphor persistence time and it is generally higher than the gate-on time, being in the range of 50 ns for SuperCam to pass from maximum intensity to zero. As can be measured for SimulCam, focusing on the 100 ns gate width series, the maximum intensity starts to decay at around 266 ns of delay, reaching zero values at 292 ns, giving an off-time of 26 ns. For Time Resolved Raman acquisitions, and despite the relatively wide gate width of 100 ns, it is possible to start the spectra acquisition before the excitation photons from the laser reach the target, collecting the spectra at the end of the gate pulse, but before luminescence photons start to appear. It is in this operational mode that the decay time of the intensifier of both instruments
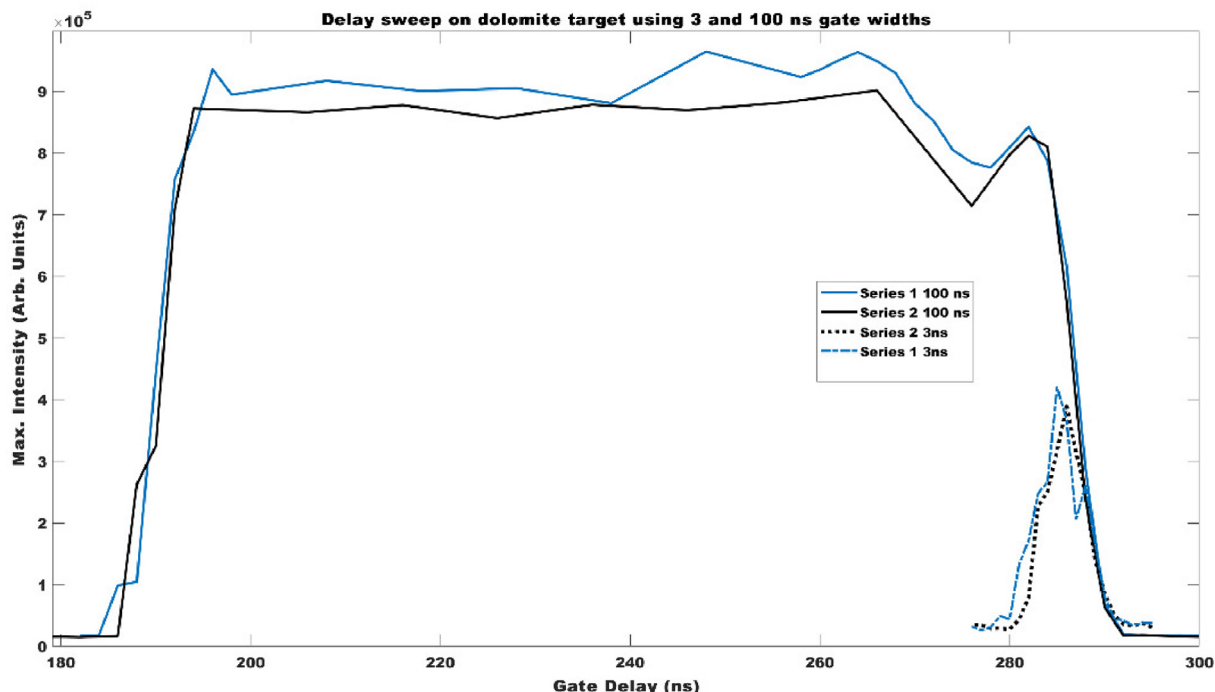
Fig. 7. Delay sweep with different gate widths. Full line for 100 ns gate widths and dashed line for 3 ns gate width, measurements were repeated, two series of data are presented per gate width. Note that for the pulse width of 3 ns this value is lower than the pulse width of the laser, decreasing the acquired energy per spectrum and the detected photons.

might have an impact in the time-resolving power. For measurements in which this kind of time-resolving measurement is not needed, and operating with minimum gate width achievable by SuperCam, for SimulCam the highest intensity was reached around 250 ns of delay, and this was set as the default delay for nominal operations, especially given the fact that for most of operation distances this value might not be needed to be updated.

Given the speed of light, during the acquisition event (gate width) the light can travel around 30 m, which introduces a sort of time-depth of field for measurements. Setting a delay of 250 ns in SimulCam, for a target at 2 m, and considering that the laser pulse gets detected after 286 ns, the instrument is collecting light before and after this laser pulse, meaning that different target planes (closer and farther) could still be measured without changing the gate delay. SimulCam would be able to cover distances from the minimum focusable distance up to distances up to 12 m (2 m of the test plus 10 additional meters) without changing the delay time. This operational particularity is also part of SuperCam's operation on Mars, as the delay rarely needs to be changed for Raman acquisitions.

3.2.6. Optimization of data acquisition procedure

As introduced in section 3.1.3, SuperCam's detector has the option to integrate on chip several discharges of the intensifier. SuperCam team evaluated the performance of the instrument using coadds during an experiment based on the analysis of the apatite target on the SCCT. This activity was performed to evaluate the optimal number of

shots to be integrated in a single CCD readout and the effect this could have on the SNR of the resulting spectra. SimulCam instrument provides the same capability, however, in SimulCam, the synchronization of the gate is set by the first trigger signal, and after a pulse train at the selected repetition rate is sent to the gate (while in Super-Cam it is the laser that triggers the gate in every discharge), the same test was emulated in the laboratory by analyzing the marble sample provided by the University of the Basque Country. In this experiment we collected several spectra using 1, 5, 10 and 20 shots integrated on chip (coadds), to achieve a total of 400 laser shots per coadd setting. This gave a total of 400 individual spectra for 1 coadd, and 80, 40 and 20 individual spectra for the rest of the settings respectively. The exposition time of the CCD was adapted in each case to give time for the coadding to occur at a repetition rate of the laser of 10 Hz. With the individual spectra we performed sequential averaging (after subtracting darks) to evaluate the SNR of the main band of marble as a function of the number of laser shots. To avoid biases, we repeated this averaging twenty times, randomizing the order of averaging each time. We did this to have a clearer idea of the SNR evolution, as well as the variability in the shot to shot.

The results of this experiment are provided in Fig. 8(a). Compared to the experiment performed on Mars by Super-Cam, see Fig. 8(b). SimulCam shows a different behavior to SuperCam in the SNR using different coadds. Using 20 coadds worked significantly worse in SimulCam than it did for SuperCam. On the other hand, both instruments
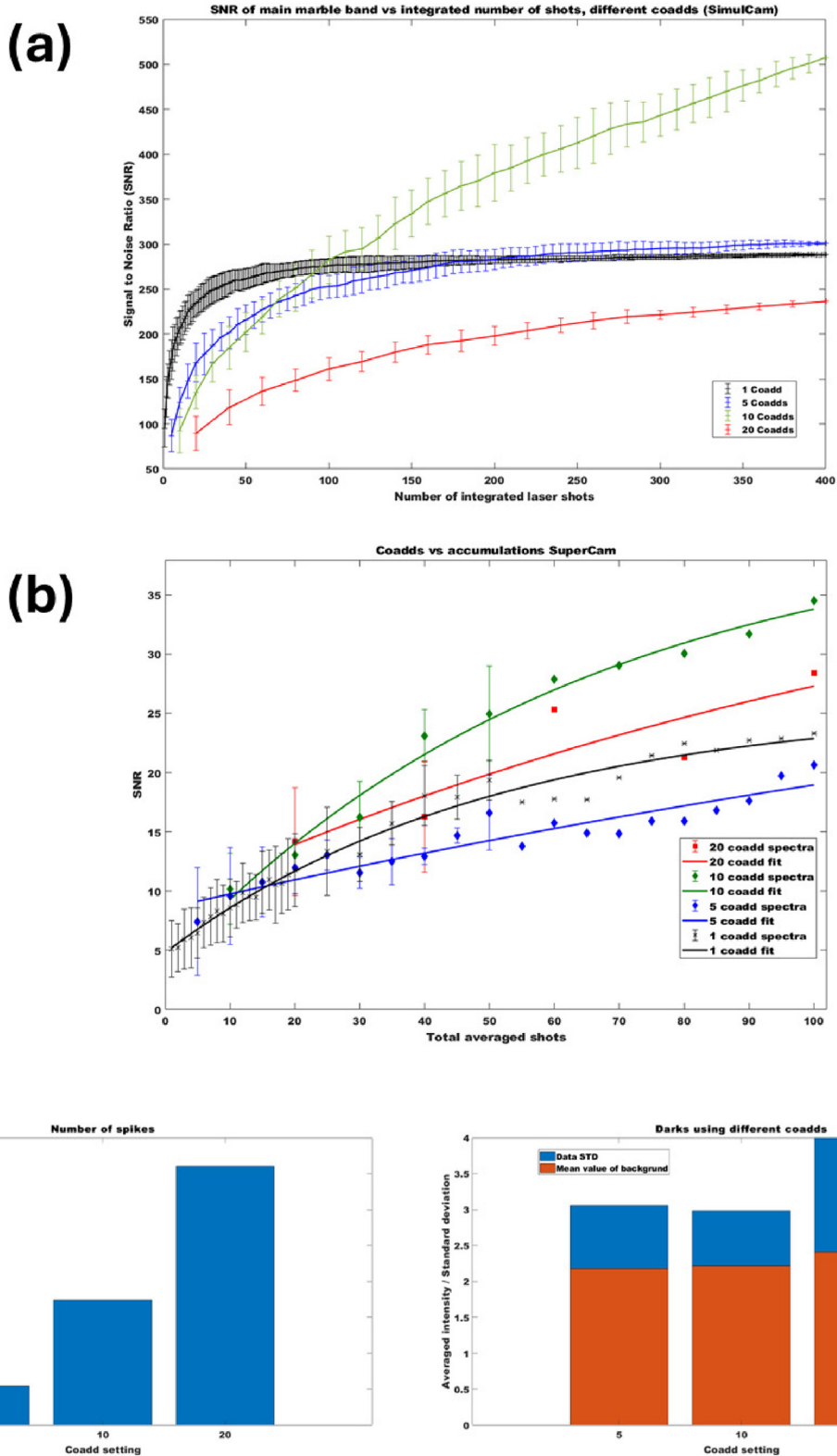
Fig. 8. (a) Coadds and SNR evolution for SimulCam, over 400 laser shots. (b) Same experiment performed on Mars by SuperCam over 100 laser shots. (c) Noise evolution and spikes in the darks depending on the number of coadds for SimulCam data.

achieved the best results when the 10 coadds setting was used. It is important to remark that for SimulCam we analyzed 400 laser shots, instead of 100, which provided the opportunity to observe how the 1- and 5-coadds acquisitions reached a point at which the SNR did not further improve despite the use of more laser shots, being this

value in SNR reached with less shots for the 1 coadd setting. For SuperCam the better performance of the 10-coadds setting was clearer almost in the first ten shots.

Focusing on the noise, Fig. 8c shows the results for SimulCam after evaluating a total of 100 darks using 5, 10 and 20 coadds. According to these results, the mean value recorded in the ROI up to 2500 cm^{-1} increased slightly with the number of coadds, as the exposure time of the CCD was also increased to fit the number coadds. Operating at 10 Hz, as SuperCam, the exposure times were 405, 905 and 1905 ms respectively. However, checking the standard deviation of the noise, the variability of the noise in the dark increased noticeably for the 20 coadds set, while it was more comparable for the 5 and 10 coadds setups. This could explain the poorer performance of the 20 coadds setting. Considering the longer acquisition times needed on the CCD to acquire 20 coadds, the dark noise will increase accordingly to a point where it is not advantageous to continue coadding. Similarly, as in SuperCam, the optimal number of coadds is set to 10. This same experiment allowed to evaluate the number of points that had a higher intensity than the average plus six times the standard deviation, considered spikes or cosmics. This number increased with the number of coadds, as the integration time of the CCD increased accordingly.

3.2.7. Evaluation of time resolved laser induced luminescence capabilities

As for SuperCam, Time Resolved Laser Induced Luminescence can be also measured by SimulCam. Therefore, a delay sweep test was performed on a fluorescent apatite sample. The results are provided in Fig. 9.

Fig. 9 clearly shows how the characteristic Raman signals of apatite disappear after the first spectrum. In this spectrum, the contribution of short decay luminescence can also be observed as a higher background. At longer delays, only the luminescence associated to Eu and Sm is observed in the spectra.

3.3. Comparison of results between SimulCam and SuperCam

After characterization activities, the SimulCam instrument was used to perform Raman analysis on a set of targets included in the SCCT, and the results were compared to those collected by SuperCam on Mars.

To emulate the Raman analysis performed on Mars, the laser power of SimulCam was set at 65 %, the spot size at 1.1 cm (ensuring a power density of 137 kW/mm^2) and the gain at 2000 (a. u.). Using these optimized parameters, spectra were acquired using 1 coadd, unless specified otherwise. This was done this way for the main reason that SuperCam performed the analyses in these targets using 1 coadd, and we had characterized the SNR well at different gains using one coadd from the experiment shown in Fig. 8. The change in acquisition parameters of SuperCam, e.g., to using coadds, happened after some of the measurements referred to hereafter.

3.3.1. SuperCam sulphur rich target (TSRICH in (Manrique et al., 2020))

The Raman spectra collected from both SimulCam and SuperCam (on Mars, during sol 149) from the sulfur rich target mounted on the SCCT (mixture of basalt and potassium sulfate) are represented in Fig. 10. The measured SNR for the main peak is 21 and 13 for SimulCam and SuperCam respectively. Background is observed in spectra from Mars and SimulCam on Earth. This background is
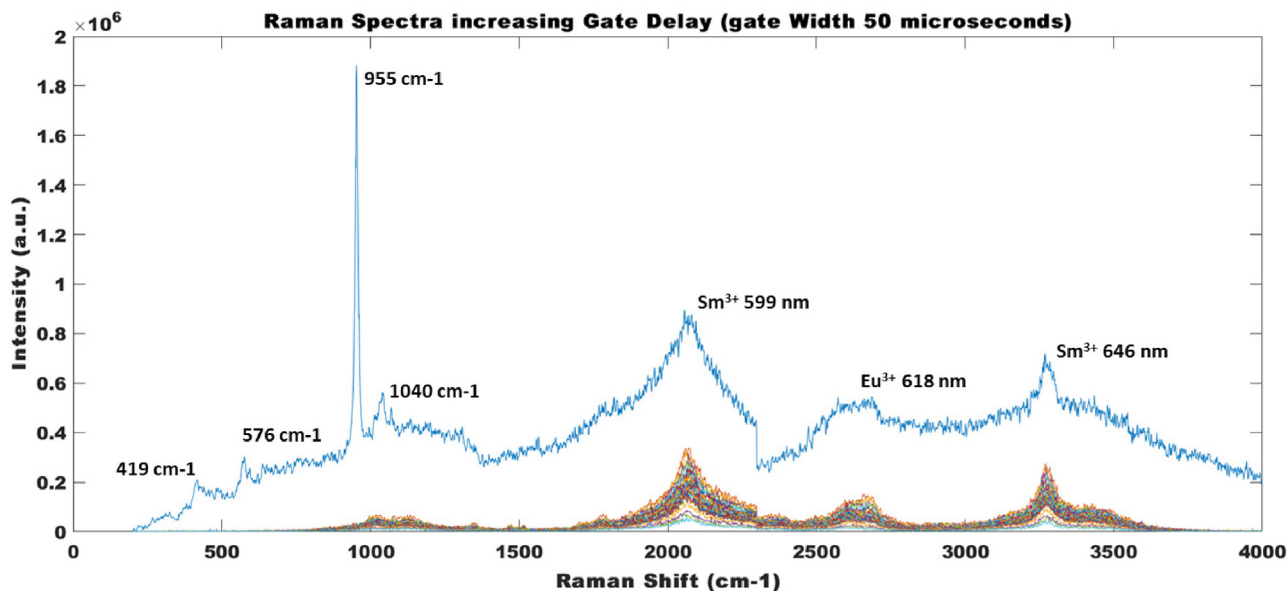

Fig. 9. Delay sweep test performed on a luminescent apatite sample by SimulCam by using a gate width of 50 μs and by increasing the delay from 0 (blue curve) to 3 ms at steps of 50 μs.
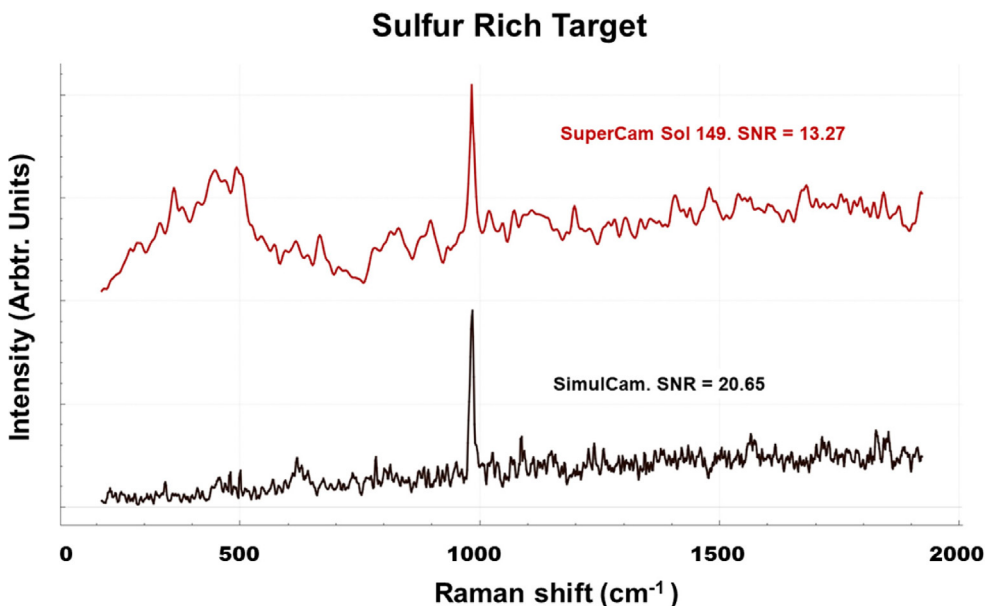
Sulfur Rich Target

Fig. 10. Raman spectra of the TSRICH target, obtained by SimulCam (black) and SuperCam (red) respectively:

more likely originated by the grained nature of the sample. Unlike for the diamond, no major differences between Mars and Earth spectra are observed. Besides the background, one main difference is the presence of a bump between 200 and 600 cm^{-1} in SuperCam spectra that comes from the Raman features introduced by the amorphous silica of the optical fiber carrying the light from the telescope to the spectrometer, as the Notch filter in the Mast Unit (Maurice et al., 2021), lets a small percentage of the Rayleigh scattered photons pass through. This was necessary to allow transmission in the UV, required for the LIBS spectra.

3.3.2. Calcite target

The Raman spectra collected from both SimulCam and SuperCam (on Mars, during sol 149) from the calcite target mounted on the SCCT are represented in Fig. 11.

This target showed considerably higher Raman signal, but also a higher background, as the fiber bump is barely noticeable in the spectrum from Mars, from 500 cm-1 to lower Raman shifts. Since this target provides a high intensity Raman spectrum, with a high background as well, the low intensity signals associated to the amorphous silica that produce the fiber bump are barely appreciable in this spectrum, as the main feature and the background are
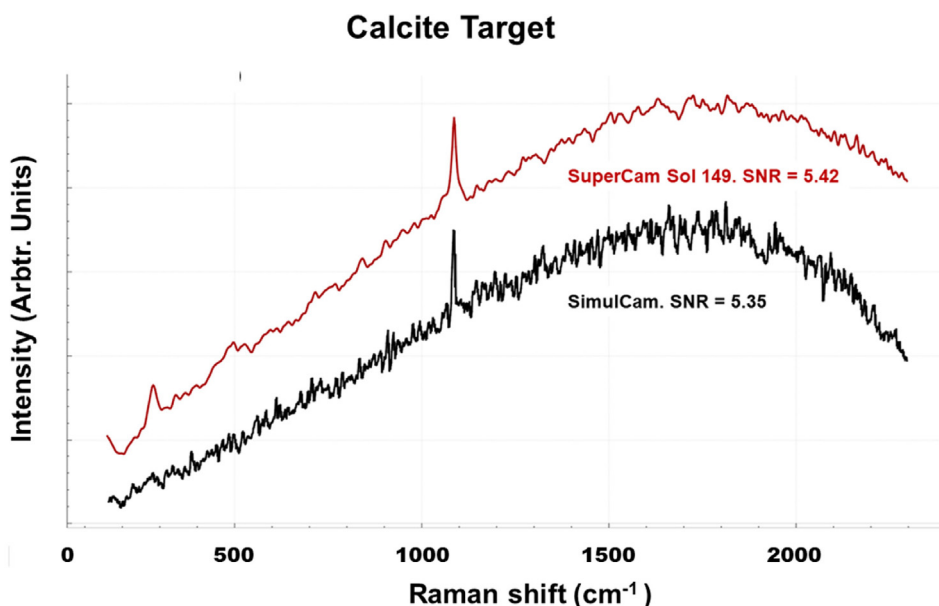
Calcite Target

Fig. 11. Raman spectra of the calcite target, obtained by SimulCam (black) and SuperCam (red) respectively:

highly intense. In this case the SNR is quite similar in both instruments, but SimulCam struggles to have a detection of the lower shift signal at 277 cm^{-1}. In both cases the background profile is quite similar despite of the fact that SimulCam is not corrected for Instrument Response Function, which might have an impact in the difference observed in lower wavelengths, closer to the edge of the track. Indeed, the IRF impact in SuperCam is characterized in (Legett et al., 2022), with a great variation between the center and the border of each track that could introduce differences in the intensity ratio of features in different spectral regions. Another factor in play could be the sensitivity of the whole detector in the margins of the intensifier tube.

3.3.3. White paint

One of the targets that have been analyzed regularly with Raman on the SCCT is the white paint of the holder. This paint is the same paint that covers Perseverance and is provided by the Jet Propulsion Laboratory (JPL). The paint provides different Raman features and is designed to be resistant to martian environment. Spectra using SimulCam were taken on the same position of the SCCT, marked as 0.6 in Fig. 12.

The spectra from SimulCam are close to those from SuperCam, with the exception of the mentioned fiber artifact. This target, with a high albedo and close distance to the Mast Unit, is one the targets producing a higher
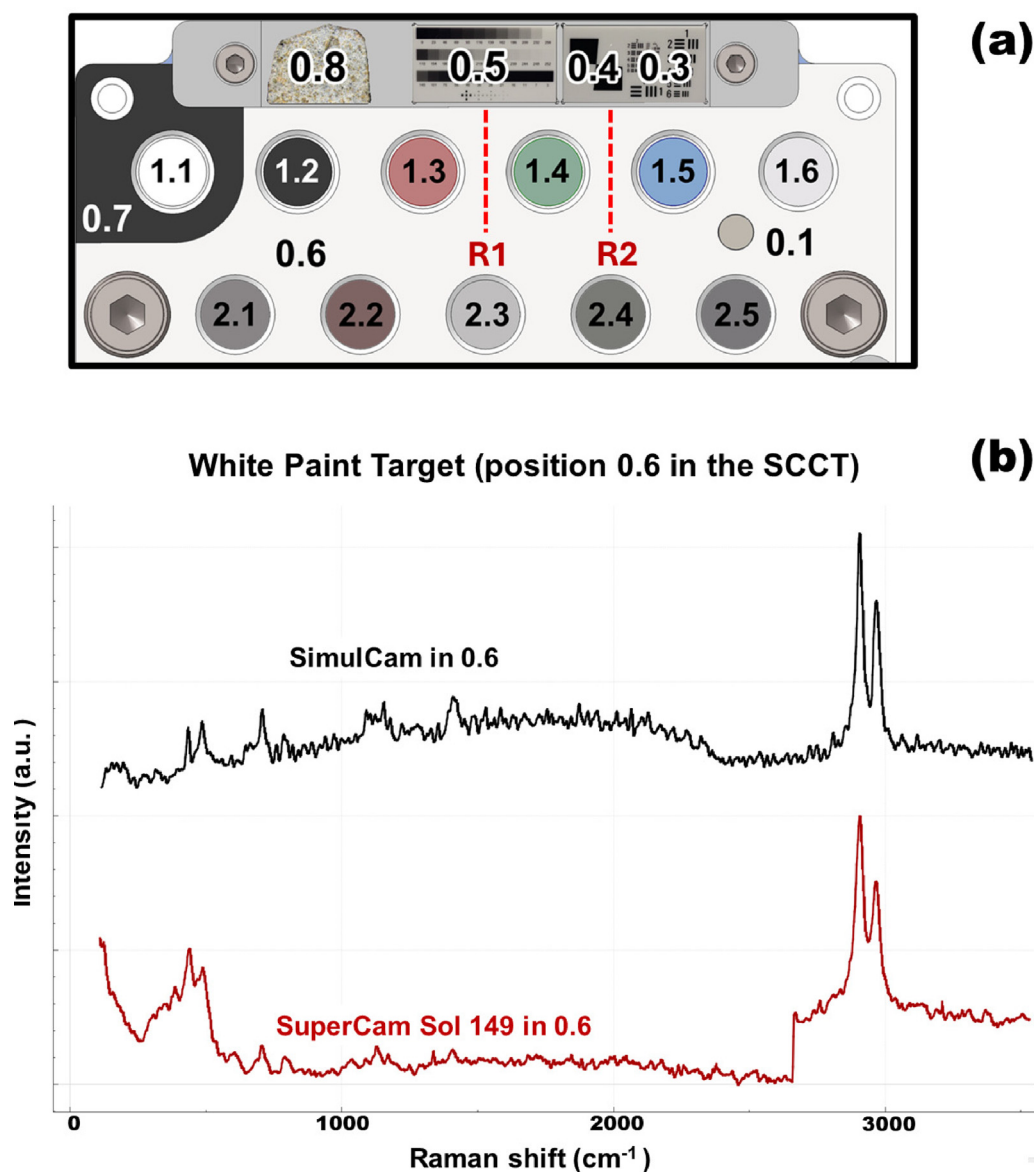

Fig. 12. (a) The white plaint that covers the holder of the SCCT is one of the targets that are regularly analyzed with Raman. Spectra are collected on position 0.6 in a wide area that is free of dust. R1 and R2 are two proposed rasters in a non-executed experiment for dust luminescence characterization. (b) SimulCam acquired spectra on 0.6 position, comparing to a SuperCam acquisition during sol 149. The fiber artifact is visible in the lower wavenumbers region.

backscattering and, subsequently, a higher interference of the fiber signals.

The white paint could be used in a proposed experiment, not executed on Mars, but that had support from Simul-Cam. The proposed experiment was meant to analyze the luminescence proceeding from the Martian dust deposited on the different targets.

SCCT passive targets (Kinch et al., 2020; Manrique et al., 2020) are protected by a magnetic system that limits the deposition of dust at their center, this is important as these reflectance standards are used for calibration of RMI color imaging and measurements of VISIR through-

out the mission. However, the magnets promote the accumulation of dust on a ring area around the targets (Fig. 13 a). Dust, in different quantities, could also be present in the PET target of the SCCT that is regularly measured to monitor ageing, or over the diamond, as both targets are not shot for LIBS and are not dust cleared by the plasma shockwave. This dust could be a factor to consider in the background evolution of different spectra. The proposed experiment consisted of performing a raster between two passive targets (R1 or R2 in Fig. 12 (a)), covering different concentrations of dust and evaluating their contribution to the spectrum of the white paint. In such
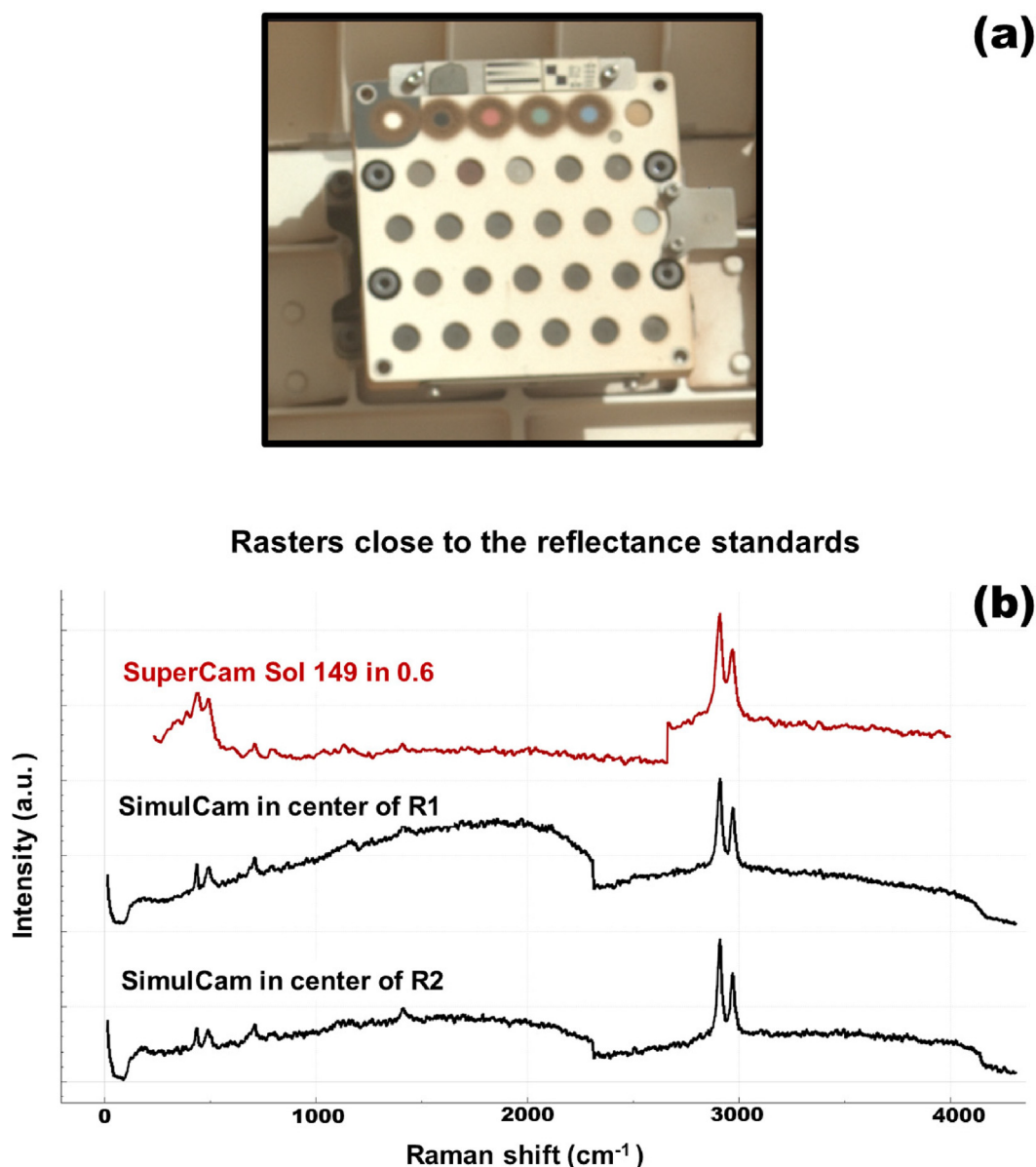

Fig. 13. Raman spectra from the SuperCam rover calibration target assembly (SCCT) and its surrogate on Earth. Spectra obtained in the center of two potential rasters for an activity on Mars, between different reflectance standards, R1 and R2 in Fig. 12(a), that present different accumulation of dust, as shown in (a) from a MastCam Z image from sol 1059. The spectrum collected on Mars by SuperCam shown in red in (b) was taken during sol 149 in the position identified as 0.6 in Fig. 12(a), a clear area under the black reflectance standard. The other two spectra correspond to acquisitions performed by SimulCam in the centre of the proposed rasters R1 and R2.

an experiment, one possible contribution could come from the reflectance standards themselves, as the laser beam diameter is greater than the analytical footprint and stray light from these targets could interfere, especially in the case of the red reflectance standard that is made using iron oxides, highly luminescent. We obtained a series of Simul-Cam spectra on the SCCT white paint (qualification model) using a beam diameter bigger than the collection area, that is, at the testing distance of 1.8 m, of 3 mm diameter for the analytical footprint, while we used 1 cm diameter for the laser spot. The targets are separated 6 mm, meaning that at both sides of the analyzed spot we had 1.5 mm of separation with the targets. As can be seen in Figs. 12 and 13, similar SNRs were achieved by SuperCam and SimulCam, but what is more interesting is the difference between SimulCam's spectra in Fig. 13, as an increase in the background appears near 2000 cm^{-1} due to the contribution of the red passive target, even with this target out of the spectrometer's nominal FOV. Also, as in previous case, artifacts associated with the optical fiber on Mars are not visible in SimulCam's data despite the high albedo and backscattering from the white paint.

3.4. Examples of support works

3.4.1. Olivine characterization

During the first Martian year of the mission, SuperCam performed multiple detection of olivine minerals at different locations. Knowing the peak position of the characteristic olivine doublet (around 820 and 850 cm^{-1}) vary depending on the degree of cationic substitution of Mg for Fe, the detailed analysis of olivine Raman spectra could provide information about the elemental composition of the mineral grain under investigation. In this sense, multiple manuscripts have been published in recent years in which the analysis of olivine crystals of known composition has been used to build calibration curves that reliably estimate the ratio between forsterite (Mg-end member) and fayalite (Fe-end member)(Foster et al., 2013; Torre-Fdez et al., 2023). These models are usually built with data from benchtop instruments, with high SNR. Having this in mind, as part of a wider work, laboratory tests were performed to evaluate those models better performing on low SNR spectra like those from SuperCam. As part of this work, synthetic olivine samples of known composition were analysed by SimulCam, replicating the SNR of Super-Cam spectra. For SimulCam data, the increase in iron in the solid solution led to a quick decrease in the SNR of the doublet (shown in Fig. 14), that may impact severely the accuracy of these models using SCAM-like data in high iron olivines. The results of the different models evaluated are presented in G. Lopez-Reyes et al. (in preparation) and helped in the selection of the model for predictions based on SCAM Raman spectra.

3.4.2. Organics detection

The SHERLOC instrument (Bhartia et al., 2021) reported several detections of organic compounds in different areas of Jezero Crater. Some of these detections were found to be associated with sulphate mineralogy (Scheller et al. 2022a). For SuperCam, and in general for Raman instruments, the presence of organics can imply a higher luminescence background and variations in its shape.

The SimulCam instrument was used to evaluate the detectability of organics of interest associated to sulphates, as reported by Mars 2020 team. Along with other instru-
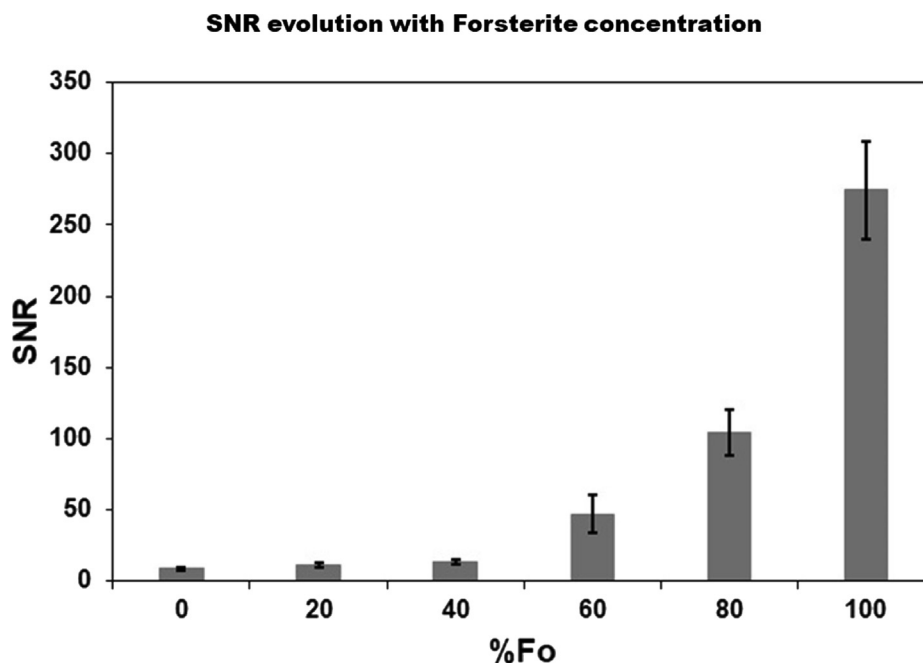

Fig. 14. SNR evolution with the concentration of Forsterite. Higher iron compositions reduce drstically the SNR, impacting different models for the calculation of Fo/Fa ratio.

ments representative of Perseverance's payload, SimulCam performed a laboratory test in which epsomite samples doped with organics were analysed and compared. Simul-Cam provided data covering the Time Resolved Raman Spectroscopy, using different irradiances and different organics, trying to correlate different background shapes observed by SuperCam in sulfates detections with possible organics, as well as direct detection of some organics of interest.

The targets were analysed by SimulCam using power density closer to SuperCam results (147 kW/mm^2) and then analysed using a higher power density (190 kW/mm^2). This was done to evaluate if higher power densities could induce changes in these targets to rule out laser induced alterations. In General, different sets of samples were prepared by T. Fornaro, as part of a wider work including SHER-LOC data. In terms of possible differences in spectra induced by the high irradiance of the pulsed laser, It was interesting to compare the behavior of some of these compounds with benchtop instruments.

Clear detection of some organic compounds was achieved using a higher irradiance, as shown in the example in Fig. 15. In this example, thymine can be directly detected using the highest irradiance setup while no shifts in the Raman features are observed.

3.4.3. PET ageing experiment

As part of SuperCam's Calibration target, SCCT (Manrique et al., 2020), a sample of PET (polyethylene terephthalate) was carried to Mars and has been exposed to the Martian environment since the beginning of the mission. This target aims to reproduce the possible ageing of organics on Mars, a process that is monitored using Super-Cam's Raman capabilities. Initial results will be published by S. Bernard et al (submitted) in a dedicated work, and preliminary results have been already shared with the community (Bernard et al., 2023). For this experiment the selected polymer was a 100 % crystalline PET, which ensured high SNR in the evaluated bands. Photochemical reactions that can occur to this material could be a Norrish Type I process (Laue and Plagens, 2005), under which the UV is absorbed by the PET to create highly reactive radicals that can end up producing aldehydes, ketones or carboxylic acid. This process does not need to react with external gases, so it is compatible with the low-pressure CO_2 atmosphere of Mars. This process could result in loss of crystallinity due to ruptures in the polymer chain induced by those free radicals. From the Raman spectroscopy point of view this could manifest in the evolution of the background, but also in changes in the profile of the two main bands at 1615 cm^{-1} and 1726 cm^{-1} (associated to
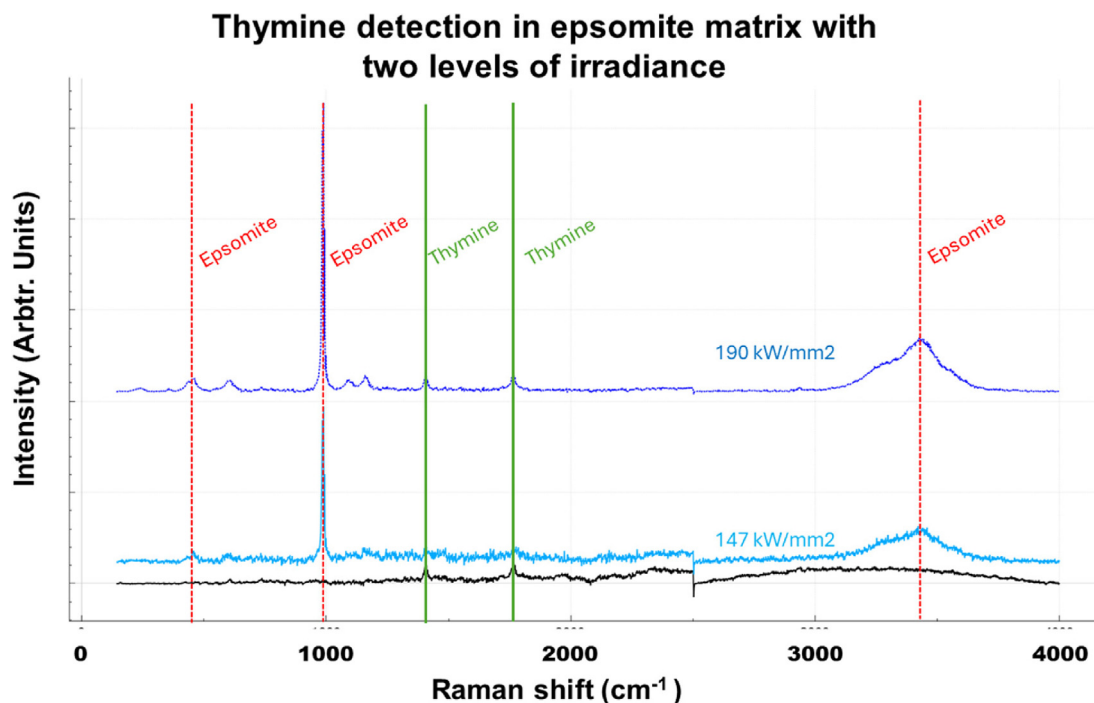

Fig. 15. Spectra of thymine. In Black we show the spectrum of the pure substance with the two main features at 1405 and 1766 cm^{-1}. These features are visible in samples of thymine adsorbed onto epsomite (blue spectra) when the higher irradiance is used (darker blue spectrum), but are not visible or too close to noise level in the spectrum using a lower irradiance (lighter blue). No shifts or effects were observed using a higher irradiance. Among the different organic compounds tested, beta-carotene offered no direct detection in the 1 % mixtures. In Fig. 16. The spectra of a pure sample of epsomite, a pure sample of beta-carotene and the 1 % mixture analyzed with both irradiances can be observed. While no direct features from the beta-carotene are observed in the spectra from the mixture, the background profile is similar in those spectra and in the spectrum from the pure organic compound, a background that is not observed in the pure epsomite. Similar behaviors are to be evaluated in the work by T. Fornaro et al. (in preparation).
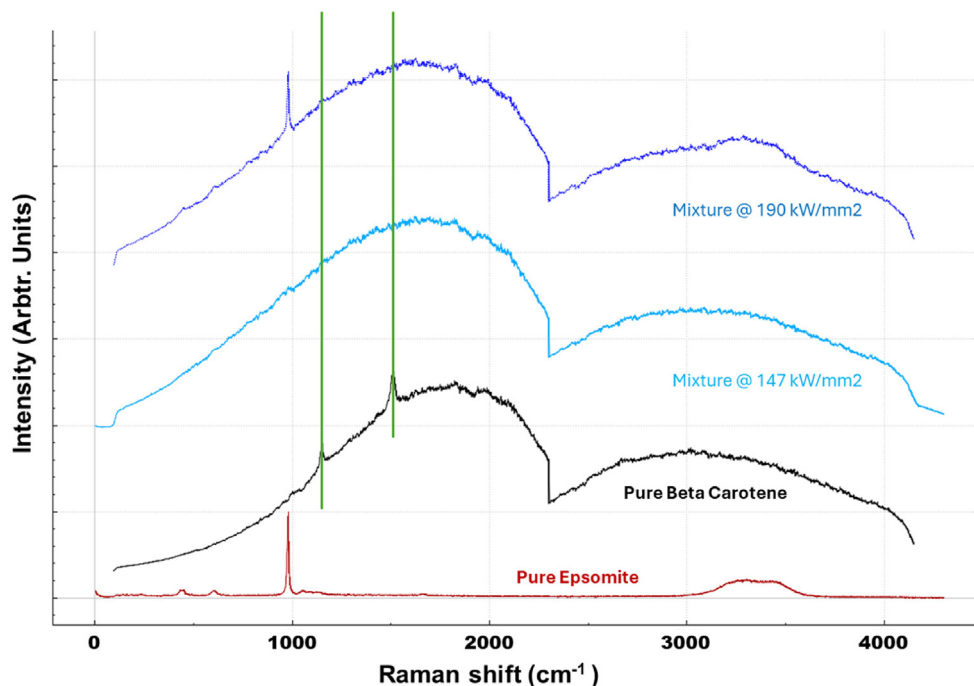
Beta carotene mixture, two irradiance levels

Fig. 16. Spectra of beta-carotene. In black we show the spectrum of the pure substance with the two main features at 1157 and 1515 cm^{-1}. None of these features were observed in the spectra of a 1 % mixture when observed with the two irradiances tested. In red, the spectrum of a black epsomite sample, where no background was observed. The background profile was similar in the three spectra with beta-carotene.

C═O), where broadening of the features in more amorphous PET has been described (Stuart, 1996), or as a result of these free radicals, examples of these changes under UV laser are described elsewhere (Rebollar et al., 2014).

SimulCam is used in combination with an environmental chamber from Linkam Scientific, to evaluate the evolution of Raman spectra of this material under different conditions of temperature when exposed to UV. In our case, the UV source was a Xenon arc lamp, which is a reliable source for UV exposure covering a wide range from 200 nm to longer wavelengths. In addition to the UV experiments we performed a series of experiments filtering out the UV to characterize possible damage induced from the more intense NIR emissions of the lamp, as compared to solar spectrum, and ruling it out. The irradiation was done in short periods, controlling the temperature of the sample and using UV-transparent windows. On the spectroscopic side, replicating SuperCam's time profile for the acquisition is key when evaluating processes involving the background, as luminescence could have time related components. Preliminary results (see Fig. 17) show how, despite replicating only a few sols on Mars, differences in the rate of the change in the background can be observed when the irradiation is done at 0 °C and −50 °C. The change in the background profile is more evident in the 0 °C series of spectra for the same irradiation, suggesting

that warmer temperatures could accelerate the degradation process. This result could be used as input when evaluating the SuperCam data that has been collected through a whole Mars year, with its seasonal changes in temperature.

The evolution of the background shown in Fig. 17 is different to that observed on Mars (Bernard et al., 2023), although this difference is currently under study as the experiments have not reached the exposure level on the SCCT's PET and both PET could be different, besides being the same commercial material (Ertalyte). Detailed data were presented as part of a Master's Thesis (Julve, 2023).

4. Discussion

After the characterization activities we demonstrated how, despite of hardware differences, the instrument can adapt to provide spectra of quality like those returned by SuperCam. Indeed, when comparing with SCCT spectra obtained by SuperCam on Mars the SNR of SimulCam is in the same range. Preliminary data showed how resolution is slightly better in SimulCam, although this resolution can be adjusted if needed to a resolution closer to SuperCam's. Nevertheless, the most limiting factor for SuperCam on Mars has not been the resolution of the spectra, but the SNR achieved and the low Raman response of
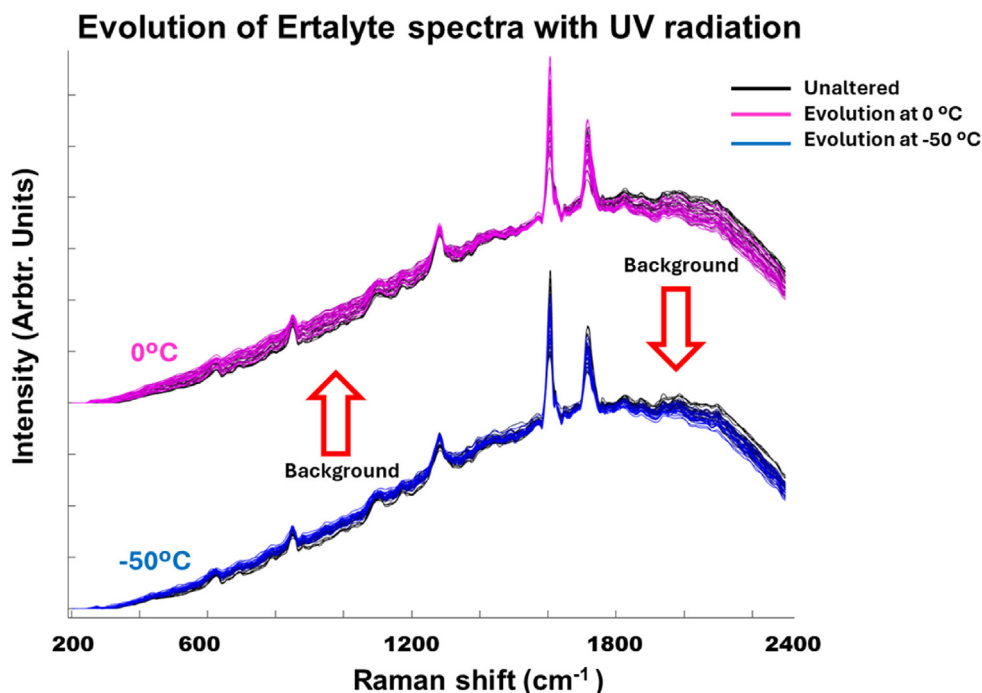
Fig. 17. Evolution of SimulCam Raman spectra of the PET with UV irradiation. Experiment has been done at two different temperatures, 0 °C and −50 °C, under dry nitrogen atmosphere and simulating the UV dosage of 10 sols on the surface of Mars. Blue spectra, from the −50 °C experiment, show a lower variation range in the background when compared to the series from the 0 ªC experiment.

the rock and soil targets on Jezero. Other issues arise from the fact that the analytical footprint of SuperCam is wide, when compared to individual grains, and Raman data corresponds to an average of the sample and not individual targets. This issue was considered elsewhere (Beyssac et al., 2023) when calculating the Forsterite/ Fayalite ratio in the olivines detected on Seitah region on Jezero, and relating that composition to LIBS measurements. Simul-Cam has a footprint that doubles that from SuperCam, but when compared to possible grainsizes of natural targets both are above 1 mm diameter at the usual operation distances. Related to this calculation, there are in the literature plenty of procedures to calculate the Fo-Fa ratio from Raman data, relating different spectral parameters with the composition of an olivine. Most of these works have been done using bench top instruments that usually have a better resolution than SuperCam or SimulCam and that operate in contact configuration, having higher SNR in their spectra. G. Lopez et al (in preparation) uses data acquired with SimulCam, along with other instruments at different conditions, for a systematic evaluation of their accuracy and their robustness when spectral quality decreases, helping in the selection of methodologies to be applied to SuperCam data.

From the time resolving characterization, besides characterizing the precise timing associated with the instrument, the behavior of the instrument was evaluated when longer gate widths are used. Operating at 100 ns width, fixing a delay to 250 ns, required to synchronize with the precise timing of the laser pulse, it was possible to collect

Raman spectra in the whole range of distances mentioned above without changing the delay, because of the temporal depth of field. Indeed, SuperCam doesn't have the need to adapt the acquisition delay when targeting at different distances. This, however, doesn't mean that time resolved studies can't be done, as the delay can be changed with more freedom. It was shown in the luminescence experiments how varying the delay of acquisition we were able to get Raman and luminescence or only the luminescence from an apatite target. Similar studies are being done on Mars by SuperCam.

Laser shots are a limited resource on Mars, as the Super-Cam laser needs breaks to cool down and prevent damage, being generally limited to < 500 laser shots per analysis. When compared to ChemCam, the inclusion of the Raman technique in the analytical tool suite, has caused SuperCam to overtake ChemCam in the number of laser shots done on Mars in less than two years of operation, indicating how demanding Raman is for standoff instruments in terms of laser shots. For this reason, laser shots should be used in a way that maximizes the outcome, and in SuperCam part of the characterization activities were dedicated to identifying the best combination of coadds that could improve the SNR of the collected spectra and evaluating the relation of SNR with the number of shots used. For SimulCam, we evaluated both, the effect of coadding (integrating several laser shots and intensifier discharges on the CCD) and the SNR gain when more laser shots are used, and we did this using the same target SuperCam used for its characterization activities. When evaluating the best way to dis-

tribute those shots, we could observe similarities to Super-Cam when it comes to distribute laser shots between accumulations and coadds, resulting on an optimal value of 10 coadds.

The characterization performed with the white marble slab showed how despite the higher power density on SimulCam, the lower ability to collect the signal back from the target compensates the final spectral quality, allowing us to find combinations of parameters that put the SNR of both instruments in the same order of magnitude for the same target. After this characterization the analyses performed using the same number of coadds and averaged spectra in some of the SCCT targets showed similar spectral quality to experiments performed on Mars by Super-Cam. The availability of the qualification model of SuperCam allowed us to plan support activities of great interest. On one hand, the fact that the SCCT EQM is safely stored and not exposed to contamination or environmental degradation, allowed us to detect a rise in the background of the diamond sample, most likely due to an ageing process of the underlying glue used for the assembly. The diamond target is transparent, not only to the 532 nm laser, but also for the UV radiation. This, in addition to a collimated excitation source, means that the laser can effectively reach the adhesive under the sample at a similar irradiance to that on the diamond. On the other hand, the diamond was selected due to its stability to environmental factors and the adhesive could be expected to be more sensitive than the diamond to these external elements. The organic target is following a similar behavior (Bernard et al., 2023), with changes induced in the target manifesting in differences in the background. In this case, SimulCam was used in combination with environmental chambers and UV lamps to evaluate the ageing process of Ertalyte on Mars. In both cases the induced changes were noted in an evolution of the background more than changes in the position or width of the Raman features. However, the change in shape of the background followed different trends on the compound on Mars and the compound in our lab, however, it is important to remark that the despite being the same commercial PET (Ertalyte), samples used for the ageing experiment came from a different provider and batch. The results suggest that the ageing mechanism is not inducing the formation of new bonds or functional groups that could introduce new Raman features. When comparing the background in other targets such as the sulfur rich target or the calcite target, we can observe a similar profile between the Earth results from SimulCam and Mars results from SuperCam and, at the same time, similarities with data previous to the launch.

SimulCam setup can help in the preparation of science activities on Mars. Raman investigations by SuperCam may be affected by the contribution of the deposited dust on the target. This could be the case of the organic target previously mentioned, being important to distinguish background changes due to structural degradation in the target

from possible contributions from the dust. SimulCam data was used in the decision making and definition of an activity that could help in this characterization, sampling the same target on Mars with different amounts of dust on top, using the white paint of the rover as target, and the variable dust deposition in the vicinity of the magnetically protected passive targets. The experiment described in section 3.3.3 helped in the selection of the location of the possible raster to be executed on Mars. The oxides used for the red glazing of the red passive target had a higher luminescence signal when compared to the rest of the passive targets, and despite of being out of the spectrometer FOV, some of this luminescence got into the collected spectra, changing their background profile. This result makes advisable the use of a different raster, closer to the green or blue passive targets, that may be less affected from luminescence not related to dust.

Different experiments described in this work showed that the SCAM-like data provided by SimulCam could be used in different works of scientific support to Mars 2020 mission. Examples of this are: the combination of different spectroscopic data for carbonate discrimination (Veneranda et al., 2023), the evaluation of Raman based methodologies for Forsterite Fayalite ratio calculation in olivines (to be published by Lopez-Reyes et al.) and similar works are in preparation for the discrimination of feldspars. These experiments are of interest given the fact that most of the methodologies that can be found in the literature part from high quality, continuous wave, bench-top instruments, that are not easily extrapolable to standoff data. Finally, one of the great points of interest of Raman spectroscopy for planetary exploration is its ability not only for mineralogy, but also for the detection of different compounds as organics. For organics, their footprint can be in the form of direct Raman features, or as the presence of short decay-time fluorescence, or both. Future work by T. Fornaro et al. will address the organic-mineral interactions from a spectroscopic point of view, at the light of recent findings on Mars (Scheller et al., 2022). In some of these abraded patches SuperCam found different background intensities that could be related, among different effects, to the presence of organics. SimulCam provided data collected with the same time parameters of SuperCam, investigating the possible effects of different organics in the Raman signal of sulfates of relevance, data to be part of the mentioned work. Besides continuing its support to Super-Cam science team, SimulCam could be used in new experiments proposed by the community or help in the development of future missions where standoff Raman could play a role.

5. Conclusions

SimulCam laboratory setup allows to obtain standoff Raman spectra at distances in the operation range of SuperCam on Mars, with some experiments shown here

at 1.8 m and others at 2 m. Limits in the operational distance are introduced by the minimum focusable distance by the collection optics and the limits of the room. Not only the distances can be replicated, but the spectral quality and other factors related to the Raman data, as the wide analytical footprint, SNR range, or time resolution power.

Performing analyses of the same targets allowed us to evaluate the combination of parameters that, despite the differences in hardware, got our data as close as possible to the Signal to Noise Ratio achieved by SuperCam in the same targets. Mimicking exactly the same behavior is quite complex, however, interesting support science can be done using combination of parameters that at least provide SNRs in the same order of magnitude of SuperCam. This confirms that the SimulCam instrument can be used to have a good representation of the performance of SuperCam on Mars.

Having a laboratory setup that can be used to obtain SuperCam-like data opens a wide range of possibilities for experimentation. Indeed, we presented examples of different works that are ongoing and use SimulCam data. The availability of this instrument is helping in the scientific support of Mars 2020 mission but results and tests could also be used for the definition of future concepts for planetary exploration using standoff Raman spectroscopy. This instrument is open for collaborations with the community in any experiments that would help for future exploration missions or helping in the understanding of data collected by Perseverance.

CRediT authorship contribution statement

Jose A. Manrique: Writing – review & editing, Writing – original draft, Investigation. **Guillermo Lopez-Reyes:** Writing – review & editing, Writing – original draft, Investigation, Data curation. **Marco Veneranda:** Writing – review & editing, Writing – original draft, Methodology. **Aurelio Sanz-Arranz:** Writing – review & editing, Writing – original draft, Investigation. **Juan Sancho Santamaria:** Investigation. **Sofia Julve-Gonzalez:** Writing – review & editing, Writing – original draft, Investigation, Data curation. **Ivan Reyes-Rodríguez:** Writing – review & editing, Data curation. **Teresa Fornaro:** Writing – review & editing, Writing – original draft, Data curation. **Juan Manuel Madariaga:** Investigation. **Gorka Arana:** Writing – original draft, Investigation. **Kepa Castro:** Writing – original draft, Investigation. **Ivair Gontijo:** Writing – review & editing, Writing – original draft, Investigation. **Ann M. Ollila:** Writing – review & editing, Writing – original draft, Data curation. **Shiv K. Sharma:** Writing – review & editing, Writing – original draft, Methodology, Investigation, Data curation. **Roger C. Wiens:** Writing – review & editing, Writing – original draft, Supervision. **Sylvestre Maurice:** Writing – review & editing, Writing – original draft, Supervision. **Fernando Rull-Perez:** Writing – review & editing, Writing – original draft, Supervision, Methodology, Data curation.

Declaration of competing interest

The authors declare that they have no known competing financial interests or personal relationships that could have appeared to influence the work reported in this paper.

Acknowledgements

References

Bernard, S., Beyssac, O., Ollila, A., Lopez-Reyes, G., Manrique, J., Le Mouélic, S., Beck, P., Forni, O., Pilleri, P., Cousin, A., Gasnault, O., Meslin, P.Y., Travis, G., Clavé, E., Royer, C., Wiens, R.C., S. M. & the S. team, 2023. Irradiation of organics on mars: evolution of the raman signal of the ertalyte target aboard perseverance. In: LPSC Conference 2023. Available at: https://www.hou.usra.edu/meetings/lpsc2023/pdf/1443.pdf.

Bernard, S., Beyssac, A.O., et al., 2023. Irradiation of Organics on Mars: Evolution of the Raman signal of the ertalyte target aboard Perseverance. In: LPSC 2023, p. #1443.

Beyssac, O. et al., 2023. Petrological traverse of the olivine cumulate Séítah formation at Jezero crater, Mars: a perspective from SuperCam onboard Perseverance'. J. Geophys. Res.: Planets 128 (7). https://doi.org/10.1029/2022JE007638 e2022JE007638.

Bhartia, R. et al., 2021. Perseverance's Scanning Habitable Environments with Raman and Luminescence for Organics and Chemicals (SHERLOC) investigation. Space Sci. Rev. 217 (4), 58. https://doi.org/10.1007/s11214-021-00812-z.

Cho, Y. et al., 2021. In situ science on Phobos with the Raman spectrometer for MMX (RAX): preliminary design and feasibility of Raman measurements. Earth Planets Space 73 (1), 232. https://doi.org/10.1186/s40623-021-01496-z.

Cousin, A. et al., 2022. SuperCam calibration targets on board the perseverance rover: fabrication and quantitative characterization. Spectrochimica Acta Part B: Atomic Spectroscopy 188.

Effenberger, A.J., Scott, J.R., Falls, I., 2010. Effect of atmospheric conditions on LIBS spectra. Sensors, 4907–4925. https://doi.org/10.3390/s100504907.

Foster, N.F. et al., 2013. Identification by Raman spectroscopy of Mg–Fe content of olivine samples after impact at 6kms−1 onto aluminium foil and aerogel: In the laboratory and in Wild-2 cometary samples. Geochimica et Cosmochimica Acta 121, 1–14. https://doi.org/10.1016/j.gca.2013.07.022.

Julve, S., 2023. Degradación de PET en ambiente Marciano: implicaciones para la detectabilidad de orgánicos en la superficie de Marte. Available at: https://uvadoc.uva.es/handle/10324/63440.

Kinch, K.M. et al., 2020. Radiometric calibration targets for the Mastcam-Z camera on the Mars 2020 rover mission. Space Sci. Rev. 216 (8). https://doi.org/10.1007/s11214-020-00774-8.

Laue, T., Plagens, A., 2005. In: Named Organic Reactions, Named Organic Reactions. John Wiley & Sons. https://doi.org/10.1002/0470010428.

Legett, C. et al., 2022. Optical calibration of the SuperCam instrument body unit spectrometers. Appl. Opt. 61 (11), 2967–2974. https://doi.org/10.1364/AO.447680.

Lopez-Reyes, G. et al., 2022. The Raman laser spectrometer ExoMars simulator (RLS Sim): a heavy-duty Raman tool for ground testing on ExoMars. J. Raman Spectrosc. 53 (3), 382–395. https://doi.org/10.1002/jrs.6281.

Madariaga, J.M. et al., 2022. Homogeneity assessment of the SuperCam calibration targets onboard rover perseverance. Analytica Chimica Acta 1209. https://doi.org/10.1016/j.aca.2022.339837 339837.

Manrique, J.A. et al., 2020. SuperCam calibration targets: design and development. Space Sci. Rev. 216 (8), 1–27. https://doi.org/10.1007/s11214-020-00764-w.

Maurice, S. et al., 2012. The ChemCam Instrument Suite on the Mars Science Laboratory (MSL) Rover: science objectives and mast unit description. Space Sci. Rev. 170 (1), 95–166. https://doi.org/10.1007/s11214-012-9912-2.

Maurice, S. et al., 2021. The SuperCam instrument suite on the Mars 2020 Rover: science objectives and mast-unit description. Space Sci. Rev. https://doi.org/10.1007/s11214-021-00807-w.

Maurice, S. et al., 2022. In situ recording of Mars soundscape. Nature 605 (7911), 653–658. https://doi.org/10.1038/s41586-022-04679-0.

Rebollar, E. et al., 2014. Physicochemical modifications accompanying UV laser induced surface structures on poly(ethylene terephthalate) and their effect on adhesion of mesenchymal cells. Phys. Chem. Chem. Phys. 16 (33), 17551–17559. https://doi.org/10.1039/C4CP02434F.

Royer, C. et al., 2024. Impact of UV radiation on the Raman and infrared spectral signatures of sulfates, phosphates and carbonates: Implications for Mars exploration. Icarus 410. https://doi.org/10.1016/j.icarus.2023.115894 115894.

Rull, F. et al., 2017. The Raman laser spectrometer for the ExoMars rover mission to Mars. Astrobiology 17 (6–7), 627–654. https://doi.org/10.1089/ast.2016.1567.

Scheller, E.L. et al., 2022. Aqueous alteration processes in Jezero crater, Mars—implications for organic geochemistry. Science 378 (6624), 1105–1110. https://doi.org/10.1126/science.abo5204.

Scheller, E.L., Razzell, J., Hollis, E.L.C., et al., 2022. First-results from the Perseverance SHERLOC investigation: Aqueous alteration processes and implications for organic geochemistry in Jezero crater, Mars. LPSC 2022.

Sharma, S.K., Ollila, A.M., et al., 2023. Performance of SuperCam's remote raman system at Jezero crater, Mars. In: 2023 Lunar and Planetary Science Conference.

Stuart, B.H., 1996. Polymer crystallinity studied using Raman spectroscopy. Vib. Spectrosc. 10 (2), 79–87. https://doi.org/10.1016/0924-2031(95)00042-9.

Torre-Fdez, I. et al., 2023. Characterization of olivines and their metallic composition: Raman spectroscopy could provide an accurate solution for the active and future Mars missions. J. Raman Spectrosc. 54 (3), 340–350. https://doi.org/10.1002/jrs.6485.

Veneranda, M. et al., 2019. Spectroscopic study of olivine-bearing rocks and its relevance to the ExoMars rover mission. Spectrochimica Acta - Part A: Mol. Biomol. Spectrosc. 223. https://doi.org/10.1016/j.saa.2019.117360.

Veneranda, M. et al., 2020. ExoMars raman laser spectrometer: a tool for the potential recognition of wet-target craters on mars. Astrobiology 20 (3), 349–363. https://doi.org/10.1089/ast.2019.2095.

Veneranda, M. et al., 2021. ExoMars Raman laser spectrometer: a tool to semiquantify the serpentinization degree of Olivine-Rich rocks on Mars. Astrobiology 21 (3), 307–322. https://doi.org/10.1089/ast.2020.2265.

Veneranda, M. et al., 2022. Analytical database of Martian minerals (ADaMM): project synopsis and Raman data overview. J. Raman Spectrosc. 53 (3), 364–381. https://doi.org/10.1002/jrs.6215.

Veneranda, M. et al., 2023. Developing tailored data combination strategies to optimize the SuperCam classification of carbonate phases on Mars. Earth Space Sci. 10 (7). https://doi.org/10.1029/2023EA002829 e2023EA002829.

Wiens, R.C. et al., 2012. The ChemCam instrument suite on the Mars Science Laboratory (MSL) rover: body unit and combined system tests. Space Sci. Rev. 170 (1), 167–227. https://doi.org/10.1007/s11214-012-9902-4.

Wiens, R.C. et al., 2021. The SuperCam instrument suite on the NASA Mars 2020 Rover: body unit and combined system tests. Space Sci. Rev. https://doi.org/10.1007/s11214-020-00777-5.